University of Groningen

Quantum transport in disordered magnetoresistive systems

Jonkers, Philip Adrianus Eduard

IMPORTANT NOTE: You are advised to consult the publisher's version (publisher's PDF) if you wish to cite from it. Please check the document version below.

Document Version
Publisher's PDF, also known as Version of record

Publication date:
2000

Link to publication in University of Groningen/UMCG research database

Citation for published version (APA):
Jonkers, P. A. E. (2000). *Quantum transport in disordered magnetoresistive systems*. s.n.

Copyright
Other than for strictly personal use, it is not permitted to download or to forward/distribute the text or part of it without the consent of the author(s) and/or copyright holder(s), unless the work is under an open content license (like Creative Commons).

The publication may also be distributed here under the terms of Article 25fa of the Dutch Copyright Act, indicated by the "Taverne" license. More information can be found on the University of Groningen website: https://www.rug.nl/library/open-access/self-archiving-pure/taverne-amendment.

Take-down policy
If you believe that this document breaches copyright please contact us providing details, and we will remove access to the work immediately and investigate your claim.

Downloaded from the University of Groningen/UMCG research database (Pure): http://www.rug.nl/research/portal. For technical reasons the number of authors shown on this cover page is limited to 10 maximum.

Download date: 05-05-2023

Chapter 8

Tunneling-Magnetoresistance

The final topic covered in this thesis concerns the current prodigy in cutting edge electronic engineering. Tunneling magnetoresistance (TMR) may be regarded as the new candidate for mesoscopic scale magnetic sensors and magnetic random-access memory elements [76]. Since TMR is relatively new (at least in industrial form), relatively little is known about these systems. In particular, little (theoretical) research is devoted to the influence of impurities on the behavior of the MR. It is the purpose of this chapter to make a contribution to the understanding of TMR and the structures which by their definition combine aspects from both GMR and TMR structures (referred to as hybrid formats, see subsection 8.2.1). In particular, we are interested in the effect of disorder on the MR since quantitatively very little is known about this feature although being quite relevant to TMR.

8.1 Introduction

The most elementary TMR system is obtained simply by replacing the non-magnetic spacer layer of a GMR sandwich configuration by an insulating (IS) layer. We write this system in short-hand symbols as: FM-IS-FM. A principal difference between TMR and GMR MMs systems is that the former type often maintains a ferromagnetic coupling between the FM electrodes whereas the latter type maintains anti-ferromagnetic coupling[1].

At the heart of TMR, as with GMR, lies the spin-polarization of the transport current due to spin-dependent scattering (see section 6.3). The fact that a ferromagnetic metal is magnetic spontaneously is due to the spin imbalance in the density of $\mathtt{d}-$states. A fraction of these polarized electrons, the itinerant $\mathtt{d}-$electrons, contribute to the (tunneling) current, as do the unpolarized $\mathtt{s}-$ and $\mathtt{p}-$electrons. As a consequence the current is partially polarized. Moreover, unlike with GMR systems where the current is predominantly carried by $\mathtt{s}-$ and $\mathtt{p}-$electrons, the current in TMR systems mainly is constituted by itinerant $\mathtt{d}-$electrons [77]. It was argued by Stearns [77] that the effective mass of these

[1] We recall that the sign of the coupling may even become irrelevant in spin-valves (chapter 7).

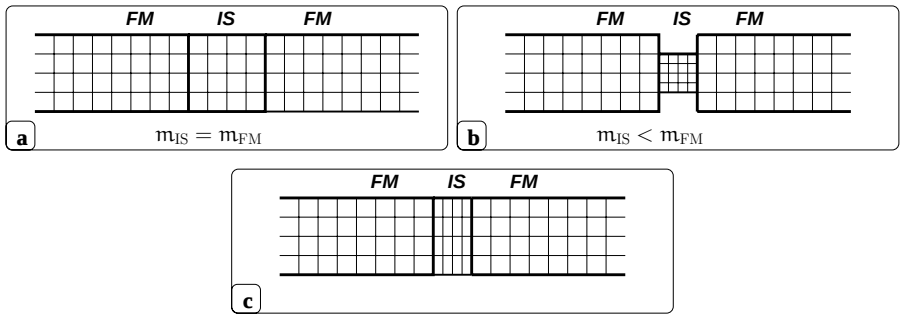

Figure 8.1: The mapping problem in a FM-IS-FM tunnel junction due to the different effective masses of the electron inside the FM layers (m_{FM}) and IS layer (m_{IS}). a. The situation where the effective masses are equal, no mapping problem. b. The masses are not-equal, in effect the dimensions of the barrier representing the IS layer (see section 8.2) shrink and induces a lattice mismatch at the interfaces. c. A partial way out to this problem is provided by only rescaling the longitudinal dimension, the transverse dimension remains untampered with, thus maintaining a proper matching at the interfaces. A drawback of course, is that the actual physical situation is compromised.

electrons inside Fe(-layers) roughly equals that of a free-electron with a mobility equal to that of $s-p$ electrons. Inside the mediating IS layer, Stearns deduced that the effective mass is significantly less than m_e. Calculations show a mass ranging from $0.2\ m_e$ to $0.4\ m_e$, see Refs. [82] and [83] respectively. On the basis of this rather wide parameter span it seems that the actual value of the effective mass is not that all important and suggests a certain stability of the results under 'variation' of the value of the electron effective mass inside the IS layer. As was indicated in subsection 3.2.2 the effective mass determines the length-scale, being proportional to $m^{*-1/2}$. Indeed, by varying the effective mass, one effectively re-scales the system. In 1D, there is a natural matching between regions supporting different effective masses. In higher dimensions, however, we run into a mapping problem as illustrated by Fig.8.1. For the dynamic method we partly remedy this difficulty by re-scaling only the longitudinal dimension. The difficulty for a complete cure arises from the implementation of the dynamic method which was not designed to handle a spatially dependent mass-parameter. On adopting different values of effective masses we may expect to find *quantitative* changes. However,it seems unlikely, simply by minor rescaling, to expect *qualitative* discrepancies to arise.

8.1.1 Discovery of TMR and Early Models

The discovery of TMR dates back to the work of Julliére in 1975 [81]. The TMR sandwich system Julliére studied consisted of a thin insulating (IS) germanium layer separating a thin iron layer from a thin cobalt layer. The thickness of the Ge-layer was then chosen to minimize the magnetic coupling between the two FM electrodes. The two electrodes have a common easy axis of magnetization but have different coercivities.

This property allows one to have an anti-parallel configuration of the magnetizations of the two electrodes when the strength of an applied magnetic field ($\boldsymbol{H}$) is chosen to lie in between the two coercive fields. The application of higher fields will then result into an alignment of the magnetizations once more. The mechanism of this basic type of TMR is analogous to that governing the GMR spin-valve structures. Intermediate magnetic fields force the magnetizations into anti-parallel mode, thus reducing conductivity. High positive or negative fields result into a parallel mode, thus increasing conductivity. The (optimistic) TMR is then found through application of Eq. (1.3) or Eq. (1.5). Similar to the spin-valve structures, the benefit of this kind of TMR set-up is that the strengths of $\boldsymbol{H}$ involved are actually of at least an order of magnitude smaller than that required for magnetic multilayer GMR systems (see section 6.1 and 7.1).

Julliére Model versus Slonczewski Model

There are several theoretical models available to explain the TMR effect which may be classified into two approaches according to the treatment of the wave function describing the tunneling electrons. The first and earliest, the Julliére model [81], is based on the tunnel Hamiltonian theory, in which the tunneling system is artificially separated into two uncorrelated subsystems by the insulating layer, each having its own Hamiltonian. This model is based on an assumption due to Tedrow and Meservey [79], stating that the tunneling current in each spin channel is proportional to the product of the "effective tunneling density of states" at the Fermi level for the given spin channel for the metals on either side of the insulator. If the system is in F-mode, Julliére's model predicts a conductance (proportional to current in the linear response regime) of

$$\mathfrak{g}_{\mathsf{F}} \propto \mathscr{D}_1^{\uparrow}\mathscr{D}_2^{\uparrow} + \mathscr{D}_1^{\downarrow}\mathscr{D}_2^{\downarrow}, \tag{8.1}$$

where $\mathscr{D}_n^{\sigma}$ denotes the density of states in layer n and spin σ. Alternatively, when in AF-mode we have

$$\mathfrak{g}_{\mathsf{AF}} \propto \mathscr{D}_1^{\uparrow}\mathscr{D}_2^{\downarrow} + \mathscr{D}_1^{\downarrow}\mathscr{D}_2^{\uparrow}. \tag{8.2}$$

The pessimistic MR ratio (also see section 1.2) follows from

$$\gamma_{\text{pes}} \equiv \frac{\mathfrak{g}_{\mathsf{F}} - \mathfrak{g}_{\mathsf{AF}}}{\mathfrak{g}_{\mathsf{F}}} = \frac{\mathscr{D}_1^{\uparrow}\mathscr{D}_2^{\uparrow} + \mathscr{D}_1^{\downarrow}\mathscr{D}_2^{\downarrow} - \mathscr{D}_1^{\uparrow}\mathscr{D}_2^{\downarrow} - \mathscr{D}_1^{\downarrow}\mathscr{D}_2^{\uparrow}}{\mathscr{D}_1^{\uparrow}\mathscr{D}_2^{\uparrow} + \mathscr{D}_1^{\downarrow}\mathscr{D}_2^{\downarrow}}, \tag{8.3}$$

which can be casted into the familiar form on using the definitions of the spin-polarized currents

$$\mathsf{P} \equiv \frac{\mathscr{D}_1^{\uparrow} - \mathscr{D}_1^{\downarrow}}{\mathscr{D}_1^{\uparrow} + \mathscr{D}_1^{\downarrow}} \quad \text{and} \quad \mathsf{P}' \equiv \frac{\mathscr{D}_2^{\uparrow} - \mathscr{D}_2^{\downarrow}}{\mathscr{D}_2^{\uparrow} + \mathscr{D}_2^{\downarrow}}, \tag{8.4}$$

giving

$$\gamma_{\text{pes}} = \frac{2\mathsf{P}\mathsf{P}'}{1 + \mathsf{P}\mathsf{P}'}. \tag{8.5}$$

Alternatively, the optimistic MR is given by

$$\gamma_{\text{opt}} \equiv \frac{\mathfrak{g}_{\mathsf{F}}}{\mathfrak{g}_{\mathsf{AF}}} - 1. \tag{8.6}$$

From Eq. (8.5) we obtain $\mathfrak{g}_{\mathsf{F}}/\mathfrak{g}_{\mathsf{AF}} = (1-\mathsf{PP}')/(1+\mathsf{PP}')$ which, substituted in Eq. (8.6), yields

$$\gamma_{\text{opt}} = \frac{2\mathsf{PP}'}{1-\mathsf{PP}'}, \tag{8.7}$$

which differs from Eq. (8.5) by a minus-sign in the denominator. Indeed, the adjective 'optimistic' serves its right well since γ_{opt} explodes if $\mathsf{PP}' \to 1$. Using the definitions (8.4) this corresponds to either the condition

$$\mathscr{D}_1^{\uparrow} = 0 \quad \text{and} \quad \mathscr{D}_2^{\uparrow} = 0, \tag{8.8}$$

or

$$\mathscr{D}_1^{\downarrow} = 0 \quad \text{and} \quad \mathscr{D}_2^{\downarrow} = 0. \tag{8.9}$$

We see from Eqs. (8.1) and (8.2) that this corresponds to a perfectly current blocking AF-mode and one blocked spin-channel in F-mode. This is the pursued ideal case of a 100% spin-polarized material. This *half-metallic* feature is explored theoretically in Ref. [83].

Though the Julliére model is admittedly simple, it is nonetheless quite successful in predicting TMR values based on current spin-polarization values. A big deficit of the Julliére model however, is that it does not account for the finiteness of the IS layer, the model implicitly assumes the FM electrodes to be completely isolated from one another. The finite width and height of the barrier representing the IS layer[1] imply that the electrodes are not at all separate physical systems. The wave-functions of the carriers in both electrodes overlap, which mandates rather than merely justifies the treatment of the electrodes and IS layer as one physical system. Indeed, the implementation of the dynamic and static method originally designed to handle CPP-GMR systems also supports the mentioned tunneling scenario. In fact, both methods can handle TMR systems without any principal modifications. The wave-numbers inside the NM layers automatically turn into attenuation constants inside IS layers. The conceptual similarity and analytical uniformity between CPP-GMR and TMR was also recognized and exploited by Mathon [84].

The earliest paper, by Slonczewski [85], which acknowledged the just mentioned proper conception of the barrier only came some fifteen years later after the advent of the Julliére model. This new type of tunneling model for the FM-IS-FM TMR format is based on the textbook solution of the free single-electron 1D Schrödinger equation for a rectangular potential barrier without disorder [2]. The approach Slonczewski adopted shows similarities with the static method as outlined in chapter 4. He imagined infinitely wide iron layers sandwiching the IS layer by introducing a spin-dependency into the wave-number of the transmitting plane waves. He then studied the dependency of the conductance on besides the barrier height and width also the angle between the magnetizations of the iron layers. The part of his result important to us, can be summarized

[1] See section 8.2.

[2] This is a sufficient condition to deploy the 1D SE representing a physical system of higher dimensionality also. Since the potential is dependent of the longitudinal (perpendicular) direction only, the multi-dimensional problem may be separated off into the 1D longitudinal direction and 1D or 2D transverse dimensions.

by the following expression for conductance (in a form adopted from Ref. [83])

$$\mathfrak{g}(\theta) = \mathfrak{g}_{fbf}(1 + P_{fb}^2 \cos\theta), \tag{8.10}$$

and

$$\mathfrak{g}_{fbf} \equiv \frac{e^2}{\pi\hbar}\frac{\kappa}{\pi w}\left[\frac{\kappa(k_\uparrow + k_\downarrow)(\kappa^2 + m_b^2 k_\uparrow k_\downarrow)}{(\kappa^2 + m_b^2 k_\uparrow^2)(\kappa^2 + m_b^2 k_\downarrow^2)}\right]^2 e^{-2\kappa w}, \quad P_{fb} \equiv \frac{k_\uparrow - k_\downarrow}{k_\uparrow + k_\downarrow}\frac{\kappa^2 - m_b^2 k_\uparrow k_\downarrow}{\kappa^2 + m_b^2 k_\uparrow k_\downarrow}, \tag{8.11}$$

where $\mathfrak{g}$ is the surface conductance per unit area, P_{fb} is the *effective* polarization of the current, $\kappa \equiv \sqrt{2m_b(U_0 - E_\perp)}/\hbar$: the attenuation constant in the barrier of a plane wave with perpendicular energy $E_\perp$; $U_0 - E_\perp$ is the barrier height as seen by the same plane wave; m_b is the electron effective mass inside the barrier of width w. From Eqs. (8.10) and (8.11) we see the sensitivity of the conductance on the barrier parameters, as opposed to the rigidity of the Julliére model. For an interesting comparison on FM-IS-FM systems of the Julliére model with the Slonczewski model and a validity discussion of both models with a more rigorous model see Ref. [86].

8.2 Model

The general model employed in this thesis (chapters 3 and 4) can also be applied to TMR systems. Following convention, we model the IS-layer by a square potential barrier with a height, denoted by $\mathcal{V}_{IS}$, with respect to the Fermi level. Though the actual form of the barrier potential is likely to deviate from the ideal rectangular shape, one may substitute the real form by a suitable (*i.e.* more-or-less equivalent) rectangular potential conform the method of Simmons [87].

8.2.1 Hybrid Formats

The introduction of the IS layer, into systems composed of FM and NM layers (GMR systems) opens the doors to a great diversity of new possible structures. These systems, composed of FM, NM and IS layers, will exhibit properties of both GMR systems and TMR systems, and are henceforth referred to as **hybrid formats** in this thesis. Indeed, as TMR is a relatively new phenomenon, many hybrid formats still remain unexplored, the justification for exploring them is then self-evident.

Since the layer make-up of the formats might get rather extensive, we introduce the following further short-hand notation: FM→F, NM→N, IS→I. Also the minus signs in between the layer-symbols will be omitted. Example: the format NM-FM-NM-IS-NM-FM-NM shrinks to NFNINFN. Note that the only role of the outer NM layers is to signify the termination of the thickness the FM layers, in effect they take over the semi-infinite property of FM layers in the FIF format. The (hybrid-) formats which have been studied to date are the following:

FIF This is the first TMR format, pioneered by Julliére [81]. The single insulating barrier (Ge) is sandwiched by two FM electrodes of different material (Fe and

Co). All aspects of this most basic of all formats were exhaustively studied both experimentally and theoretically, see *e.g.* Refs. [81]- [94].

FNIF The insulating layer is separated from one of the FM electrodes by introducing an NM layer, it is argued in Ref. [96] that this measure increases MR and magnetic field sensitivity.

FIFIF The most elementary double barrier system, studied in *e.g.* Ref. [95]. The main conclusion of this paper is that in this double barrier structure the absolute value of MR is substantially enhanced as compared to the FIF single barrier system. Negative and positive MR can be achieved by adjusting the bias voltage.

FIF$_1$IF$_2$IF This triple-barrier system is argued to be viable for very large MRs (2000%) due to the formation of two spin-dependent quantum wells inside F_1 and F_2 [100].

NFIFN The single barrier sandwiched by two FM layers each connected to NM electrodes. This is a predecessor to the hybrid format. An implication of the inclusion of NM bordering electrodes into the analysis is that the calculated MR shows dependency on the thickness of the FM layers. In Ref. [97] it is argued that the MR oscillates with the thickness of the FM layers and may reach a very large value under suitable conditions. The mechanism responsible for the oscillations in MR turns out to be a very basic quantum property and will be revealed later on in this chapter.

FINIF The double barrier sandwiching an NM layer. In turn, the double barrier is sandwiched by two FM electrodes. This is the first example of an hybrid format, studied in Ref. [98]. The main finding given in this paper is that with increasing the NM thickness, the MR exhibits (analogous to the previous format) oscillating behavior. The MR can allegedly be enhanced by selecting FM layers with high spin polarization and by controlling the NM layer thickness finely.

In this thesis we will study four types of hybrid formats of which three types were not previously studied. A vulnerable point in most of the previously discussed hybrid formats is that the outer FM layers are implicitly assumed to be semi-infinite. In real structures however, this cannot be valid since the systems are of finite dimensions. The FM layers are of finite dimensions and are connected to external NM electrodes. The only format which properly acknowledges this property is the NFIFN format given above. A consequence of the 'inclusion' of the FIF system by NM electrodes is that, through additional (spin-dependent) scattering at two new exterior interfaces, this generally leads to an increase in MR as compared to the FIF format. Secondly, the MR now becomes dependent on the thicknesses of the (outer) FM layers. In fact, the MR turns out to be oscillatory in the thicknesses of these layers, as was already mentioned above (also see Ref. [97]). Analogous to GMR systems, the distance between the FM layers in hybrid formats is assumed to be chosen such that the coupling of the magnetizations in the FM layers be naturally anti-parallel. This condition forbids the variation of the distance between the FM layers to arbitrary extent, instead it is reduced to relatively narrow intervals. Thence, we will mainly vary the thicknesses of the FM layers. Note

that the hybrid formats are different in character from the historic FIF format in that with the latter format the magnetic coupling is naturally ferromagnetic rather than anti-ferromagnetic. In these FIF systems the two FM layers have different coercivities which enables one to pin the magnetization of one layer and rotate freely the magnetization of the other layer (see subsection 8.1.1). In hybrid formats however the FM layers are assumed to be constructed out of one material only, in this thesis we confine our attention to Fe and Co only. The representation of the NM layers appearing in the hybrid formats have either an exclusive Cr or Cu character in case of having Fe or Co FM layers, respectively.

The next hybrid formats were studied in this thesis:

NFIFN The most elementary hybrid format. Previously studied by Zhang *et al.* [97], also see the fourth of the previously formats.

NFNINFN This format is obtained if NM layers are inserted between the FM-IS and IS-FM bilayers. The thickness of the NM-IS-NM layer sequence must be chosen such as to maintain an anti-ferromagnetic coupling between the two FM layers. The idea behind introducing the extra NM layers is to create additional spin-dependent band-bottom potential wells serving to 'trap' the wave-function in between the FM and IS layers. If the system is in F-mode, the levels of the band-bottom potentials cause only one of both spin-channels to be trapped effectively. When the system is in AF-mode however, each spin faces a trap though. The trap for one spin is located at a different side of the barrier as compared to the other spin. As a consequence one of the F-mode spin-channels and both the spin-channels in the AF-mode system experience a heavy reflection, which then leads to high values of MR.

Due to the typical location of these potential-levels the effect is expected to be larger for Co layers, where the levels tower above the level of the NM layers, than for Fe layers, where the levels are 'submerged' (also see Fig.8.2). A second motivation for this measure is to facilitate extra room for impurities. In case of having Fe FM layers and Cr NM layers such measure is expected to have a positive effect of impurities on the MR since annealing FeCr GMR multilayers increases MR (see chapter 6). We may, at least, hope to find a lessening of the reducing effect on the MR of impurities.

NFNFIFNFN If FM layers are added to the exterior of the first format mentioned in this list, we obtain the present format[1]. The motivation for taking such a step is again to facilitate extra space for impurities.

NFNFNINFNFN The last format treated in this thesis arises if extra NM layers are inserted adjacent to the IS barrier in the previous format. The motivation is two-fold and identical to that given in the discussion of the second format.

[1]The format is thought to be enclosed by NM electrodes.

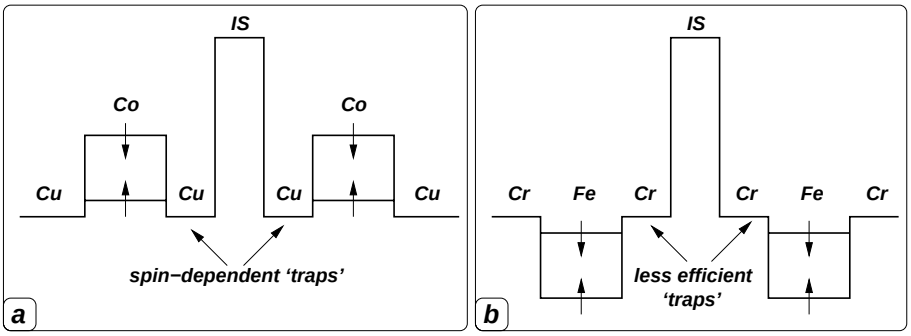

Figure 8.2: The band-bottom potential profiles of NFNINFN hybrid formats illustrating the 'trapping'-mechanism responsible for an increase in MR in particular for Co FM layers (a) compared to Fe FM layers (b). Both formats are in F-mode.

8.2.2 Basic Format

Aside from the previously discussed hybrid formats we will also briefly focus on the basic FIF format using the static 1D method of chapter 4 and calculate the MR as a function of barrier height and thickness. The acquired data then serves as a means for comparison with the more complex hybrid formats.

The system of interest describes the original Fe-Ge-Co tunnel junction pioneered by Julliére [81]. The 'incoming' static waves enters the Fe layer and by the FM nature of the electrode are given a spin-dependent momentum. The 'outgoing' or transmitted waves are defined on the Co layer. Since the Fe and Co layers are modeled by different band-bottom potentials the momentum of the wave changes in going from Fe to Co. The transmission coefficients are defined as, following convention, the outgoing current divided by the incoming current. In case of having NM terminals the momenta of the incoming wave cancels out with that of the transmitted wave to give the usual transmission coefficients of the form $|t|^2$ (see chapter 4). On having FM terminals, however, we obtain transmission coefficients of the form $|t|p_2/p_1$, with p_1 and p_2 the momentum of the outgoing and incoming wave, respectively. Also note that these momenta are spin-dependent and that the outgoing momentum also depends, by set-up, on the mode of system (AF-mode or F-mode) (also see Fig.8.3).

The results of the calculations are given in Fig.8.4. The effective mass of the electrons in the Ge barrier was set at $m^* = 0.082\ m_e$ [99]. Fig.8.4 basically exhibits two features: the MR is a decreasing function of the width of the insulating layer and increasing function of the barrier height.

The former feature, is a general property not specifically owed to quantum mechanics. To prove this, it suffices to advance a more simple non-quantum model which features the same property. Consider a modification of the resistor model as given in section 6.2. To represent TMR systems, we insert an additional resistor with value r_{IS}, representing the insulating layer, in between the resistors that represent the FM layers. We assume resistance of the resistor to be proportional to its length (the width of the IS layer).

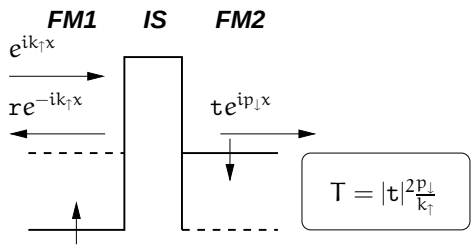

Figure 8.3: Illustration of the redefinition of the transmission coefficient in case the terminals are of FM nature. The F_1IF_2 format is in AF-mode. A spin-up wave enters from the left with momentum $k_\uparrow$ and is partially transmitted with an altered momentum $p_\downarrow$, yielding the expression for the transmission coefficient T as given in the figure.

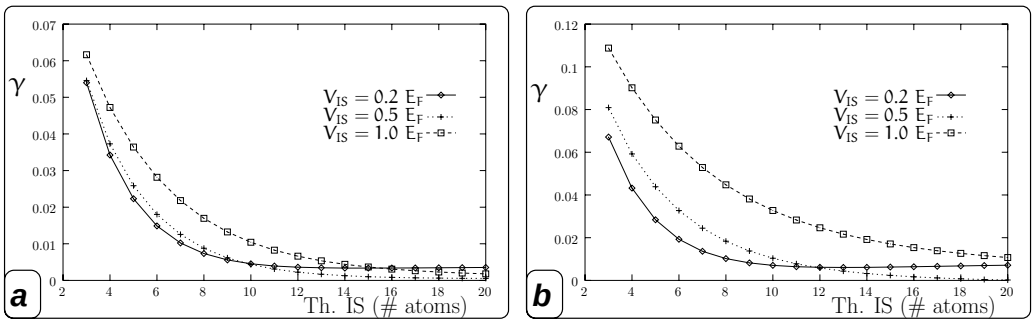

Figure 8.4: The original Fe-Ge-Co tunnel junction given a traditional analysis. The band parameters of the Fe layer were taken from Expr. (6.18). a. The results on MR with Co band-parameters of Expr. (6.20). b. The MR obtained with Co band-parameters of Expr. (6.21).

Then repeating the same steps of section 6.2, we end up with a modified expression for the MR

$$\gamma = -\frac{\tilde{\beta}^2}{1-\tilde{\beta}^2} \quad \text{where} \quad \tilde{\beta} \equiv \frac{\beta}{1+\frac{1}{2}\mathfrak{r}_{IS}/\bar{\mathfrak{r}}}. \tag{8.12}$$

As the layer-width increases, then so does $\mathfrak{r}_{IS}$ which, in return, reduces $\tilde{\beta}$ and γ. Hence we have shown that the reduction of MR in a TMR system with the width of its insulating layer is not exclusively a quantum property.

The second property, the increase of MR with the barrier height, however is a true quantum (tunneling) property of the barrier. Consider the system to be in F-mode. Recall from elementary quantum mechanics that the amplitude of the wave function decays, in the process of tunneling through a barrier, as $e^{-\sqrt{\mathcal{V}_{IS}-\mathcal{E}_\perp}\,d}$, with d being the barrier thickness and $\mathcal{E}_\perp$ the perpendicular (longitudinal) energy. If the barrier is low (but still above Fermi level), the channels with the highest $\mathcal{E}_\perp$ will suffer the least of

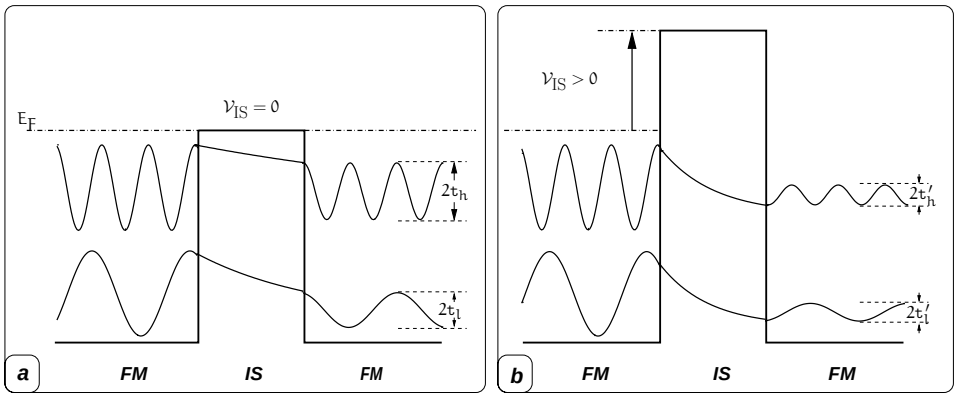

Figure 8.5: Illustration of the physical mechanism responsible for the increase in polarization of the current (conductance) and hence MR, as a reaction to a boost in $\mathcal{V}_{IS}$. Consider the tunneling of two plane-waves, one with high and one with low (perpendicular) energy, through a barrier. a. The barrier is low, meaning that the discrepancy in rates of transmission between high and low energy channels, relatively given by $|t_h|^2$ and $|t_l|^2$, is greater compared to the high barrier case, given in sub-figure b with the rates of transmissions given by $|t'_h|^2$ and $|t'_l|^2$. In summary, $|t_h|^2/|t_l|^2 > |t'_h|^2/|t'_l|^2$.

decay through the barrier and will contribute most significantly to the tunneling current. The channels with the lowest $\mathcal{E}_\perp$ will rapidly decay inside the barrier and will contribute least significantly to the current. The effect of the barrier, on increasing its height $\mathcal{V}_{IS}$, is to reduce the differences in transmission of the tunneling current between the various channels. That is, the channels with highest $\mathcal{E}_\perp$ loose significance while the channels with low $\mathcal{E}_\perp$ relatively gain significance. In due process, the total *number* of channels gradually gains relevance over the privileged highest $\mathcal{E}_\perp$ channels. A graphical support for this line of argument is presented by Fig.8.5. Since the system is in F-mode, this means that the number of majority spin-channels exceeds that of the minority spins. Therefore, increasing $\mathcal{V}_{IS}$ results in an increasing discrepancy between the transmitted currents due to the majority and minority spins. Hence, the current and thus conductance gets more polarized (in favor of majority spin).[1] When the system is in AF-mode, only the channels with perpendicular energy above the minority spin level contribute to the tunneling current. The number of channels contributing to the current then is spin-independent and the tunneling current is roughly equal for both spins. The increase of barrier height then does not lead to an increase in spin-polarization of conductance. In summary, increasing the barrier height increases the polarization of the current (conductance) in F-mode which, in turn leads, by increasing the difference between F-mode conductance and AF-conductance, to an increase of MR.

[1] Note that this consequence is relative, the actual magnitudes of current and conductance drop.

8.2.3 Sub-ensembles

The way the 2D dynamic method is set-up here is identical to the set-up of the GMR systems except for one subtle but significant modification. Consider the definition of the multi-Gaussian Eq. (3.45), it turns out that in tunneling formats the transmission is strongly dependent on the set of random phases $\{\phi_n\}$. Each set of random phases gives a significantly different transmission than the next, the standard deviation from the average transmission is around 20-30 percent.

The solution to this difficulty is provided by introducing **sub-ensembles**. A sub-ensemble consists of a set of equivalent multi-Gaussians, with each member having its own unique set of random phases $\{\phi_n\}$. The multi-Gaussians are launched in on the system[1] at hand separately. The accumulated transmission coefficients then serve as the transmission coefficient representative to that system. The above steps are then repeated for the entire ensemble of systems in the usual manner (chapters 5 and 6). The average of the accumulated transmission coefficients is then used to obtain the magnetoresistance. The criterion on the size of the sub-ensembles is reasonable convergence of the magnetoresistance. In practice, a size between 8 to 16 seems to suffice. A big drawback of having to invoke the concept of sub-ensembles is that the required computing time is proportional to the size of the sub-ensembles, in practice this means that this amount of time easily increases by a factor of ten as compared to the single-member subgroup case.

We stress though, that this effect is exclusively pronounced for tunneling systems, the fluctuations in transmission of GMR seem to be of an order of a magnitude small. We therefore did not consider it to be worth the effort to apply the concept of sub-ensembles to GMR systems too.

8.2.4 Disorder

Since the role of disorder in TMR systems has not yet received much attention, we consider it worth while to study its effect on TMR systems. Disorder enters the model in the two distinct ways as mentioned in section 1.3: By introducing finite-sized spin-dependent potential bars (representing impurities) and a non-uniform variation of the layer thicknesses. The impurities reflect the occurrence of foreign stray atoms in, the otherwise, pure system and the procedure of introduction was already discussed in subsection 6.3.1. It is argued (see *e.g.* [94]) that disorder in the form of impurities has a detrimental effect on the value of TMR, this may indeed be the case for simple TMR formats (such as FM-IS-FM) but for GMR-TMR hybrid structures this may very well be different as *e.g.* the GMR is seen to increase with the degree of disorder for FeCr MMs (see chapter 6). Therefore it might be rewarding to explore the influence of disorder on these hybrid structures.

The CPP character and their modest size make impure TMR systems very well suited for treatment by the dynamic model. In addition, since the 1D static model with impurities proved to be ill-suited for this matter[2] the value of the dynamic model increases even further. However, the validity of the 1D static model in the clean limit still remains.

[1] With 'system' is meant here a system with an, in principle, unique impurity configuration.

[2] The rather obtrusive character of the impurity modeling in the 1D static model is held responsible

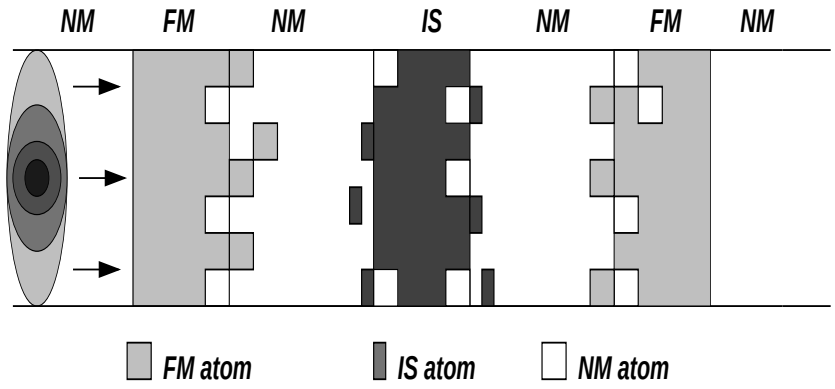

Figure 8.6: Illustration of a 2D disordered hybrid format (NFNINFN) system.

As with GMR systems, disorder, in the form of interface roughness (see subsections 6.1.3 and 6.3.1), is introduced by annealing the samples. It is interesting to note that annealing serves a two-staged role in TMR systems. It is found experimentally [94] that on exposing the TMR samples to short annealing up the MR ratio improved considerably. The temperature leading to an optimum MR was inferred to be around 230°C beyond which the interfaces began to deteriorate. The improvement in the interface properties upon annealing has been attributed to barrier homogenization [94] and better magnetic properties of the FM films near the interfaces. Other factors may include reduction of the defect density in the barrier and sharpening of the FM-IS interfaces. Some of these suggestions are supported by the slight (inferred) increase of the barrier height as well as the large increase in MR. Beyond 230°C, annealing will cause degradation of the interfaces in the sense of inducing the familiar mechanism of interlayer atomic diffusion (see subsection 6.3.1).

Since our clean TMR systems already correspond to the optimum anneal result by construction, we will be restricted to implement the second stage of annealing only. Just as with GMR systems interface impurities are conceived as foreign stray atoms originating from a neighboring layer migrated into the host layer. Since we now have three types of layers, FM, NM and IS, we now also have three kinds of (interface) impurities, see Fig.8.6 for a typical depiction of a disordered hybrid system.

Disorder within the insulator was the subject of recent theoretical investigation by Tsymbal and Pettifor (T&P), see Refs. [101], [102] and the review article Ref. [94]. In the first article T&P introduced disorder through a random fluctuation in the on-site potentials within the insulator. Then, through calculating the conductances of both spin channels the polarization of the current was found, from which they calculated the MR

for the unrealistic results obtained for the impure 1D TMR systems. It was observed that the strongly fluctuating TMR rose far beyond the "clean" value with standard deviations greater than the actual TMR ratios. For this reason we abandon the 1D impurity implementation of the 1D static model and confine our attention strictly to clean 1D systems.

by the Julliére formula (8.5). Their main finding was that disorder induces the formation of highly conducting resonant states connecting the two metals through the insulator. This effectively reduces the height of the tunneling barrier which then reduces the spin-polarization of conductance and hence the MR. They further argued that the effective height of the barrier decreased still as the width of the disordered insulator was further increased.

In their second article [102], T&P introduced impurities next to the random on-site potential fluctuations. The on-site potential of the impurities was fixed but distributed randomly across the insulator. By calculating the DOS at both sides next to the insulator they again estimated the MR through invoking the Julliére formula. They found that the introduction of impurities lead to the formation of an impurity miniband within the band-gap of the insulator. The latter mechanism provides an additional contribution to the conductance next to the resonant state formation due to disorder. Aside from one special case, they found that the polarization of the conductance and hence MR decreased with impurity concentration. In light of the barrier potential picture, this scenario is equivalent to the formation of **corridor** like states through the conductor in which tunneling can proceed with greater ease. The formation of these corridors strongly increase conductance and, in fact, will dominate over the impurity-free contribution to the tunneling conductance. As the impurity level increases, then so does the formation of corridors. Since corridors in effect lower the effective barrier height, the MR will decrease with increasing impurity levels.

From the findings of T&P we may infer what the effect will be if, the otherwise pure, tunneling system is provided with impurities. Firstly, impurities that model diffused atoms from the insulator into the metal layers adjacent to the insulator will feature insulating properties. Hence their presence will effectively widen the barrier, and have a decreasing impact on the MR. Secondly, impurities that model diffused metallic atoms into the barrier will help create relatively high conductive corridors with a much lower effective barrier height. There is however a subtle discrepancy in character of metallic impurities inside the insulator T&P used and the ones we use. T&P parameterize these impurities with a spin-*in*dependent constant on-site potential. In our model, whether or not these impurities are represented by spin-dependent or spin-independent potentials is dependent on the character of the layers next to the IS layer. If the neighboring layers of the IS layer are ferromagnetic we define the on-site impurity potential for majority spins by an amount of two times the magnitude of the magnetization lower than that for minority spins (Zeeman splitting). On the other hand, if these layers are non-magnetic we define the on-site potential spin-independent (analogous to the paper of T&P). In the former case, this measure introduces a subtle spin-dependency into the corridor tunneling mechanism, giving a slight increase in MR as compared to the latter case, producing spin-independent corridors.

In summary, the effect of impurities modeled here, will have a negative impact on the MR by effectively widening the layer and lowering the barrier height. The effect of impurities within the insulator will depend somewhat on the type of these impurities, the strong decreasing effect of NM impurities will be milder with FM impurities.

8.2.5 Algorithms of Study

In the types of hybrid formats taken up here, the character of the FM layers uniformly is either iron-like or cobalt-like. The NM layers mimic either chromium or copper. To maintain contact with the GMR systems, the FM-NM combination remains either FeCr or CoCu. For the usual band parameters that go with them, see section 6.3 (we have chosen the band-parameters of Expr. (6.20) for the Co layers).

The FM layers appearing in the hybrid formats modeled here, are thought to be of identical make-up analogous to the MMs GMR systems treated in chapter 6 and 7. By the same mechanism as in MMs, this will lead to a negative MR. We stick to F/AF-mode type of MR in this thesis and quantify MR by utilizing Def. (6.1).[1]

We are interested in two matters of investigation concerning hybrid formats. Firstly, the dependence of the MR on the thicknesses of the layers that constitute the format, especially the FM layers. Furthermore, we will try to determine the conditions which lead to the highest values of MR. The method to study this, is an application of the 1D static method as outlined in chapter 4. Secondly, the dependence of the MR on the impurity concentration. For this purpose we use the 2D dynamic method of chapter 3. We will vary the height of the potential barrier $\mathcal{V}_{\mathrm{IS}}$ leveled from 0 to $1\ \mathsf{E}_{\mathsf{F}}$ above Fermi level. We assume this range to be sufficiently big to cover all possible and actual barrier heights.

After the layer-configuration has been defined, each format is subjected to the following two algorithms of study. In either program, each layer in every format is allowed to vary in some predetermined thickness-interval, we call this set of ranges the **thickness spectrum**. To respect the demand for having an anti-ferromagnetic coupling between the magnetizations of consecutive FM layers we will primarily vary the FM layer thicknesses and keep variation of the thicknesses in the other layers to a minimum.

In the first program the thicknesses of the NM layers and IS layers are set fixed. The MR as a function of the thickness of the FM layers is then calculated according to the following scheme:

1. The height of the IS barriers is set at Fermi level ($\mathcal{V}_{\mathrm{IS}} = 0$).
2. The thicknesses of all NM and IS layers assume initial values from the thickness spectrum.
3. The thicknesses of all FM layers assume initial values from the thickness spectrum.
4. The MR is calculated and recorded.
5. The thicknesses of two of the FM layers are increased simultaneously until the spectrum has been ran through, in the latter case we proceed with the next step otherwise we return to step 4.
6. The thicknesses of the NM and/or IS layers are changed as permitted by the thickness spectrum, we return to step 3 if the spectrum has not been completed or proceed with step 7 otherwise.

[1] If we would consider the angular variation of MR, we would prefer Def. (7.2) over Def. (7.1).

7. The height of the IS barriers is increased by some fraction of E_F until the height has reached 1 E_F above Fermi level, we then terminate or continue by returning to step 2 otherwise.

The impurity aspect of hybrid formats is studied according to the following optimization algorithm:

1. The height of the IS barriers is set at Fermi level.
2. All layer thicknesses assume initial values as prescribed by the thickness spectrum.
3. The MR is calculated and recorded.
4. The thicknesses of the layers are changed allowed by the thickness spectrum. Until the spectrum has been ran through we return to step 3 or proceed with step 5 otherwise.
5. The resulting spectrum of MRs is sorted from high to low.
6. The height of the IS barriers is increased by some fraction of E_F until the height has reached 1 E_F above Fermi level, we then proceed with step 7 or return to step 2 otherwise.
7. The average[1] spectrum of sorted MR is calculated and yields the average MR 'top 10'.
8. The configurations of the MR top 10 qualify for further investigation using the dynamic model with the sub-ensemble facility to study the influence of impurities. A criterion for a configuration to proceed to 2D analysis is that it has to offer room to an extensive number of impurities, *i.e.* the system should not be too small.

8.3 Results

In short, our objective was to study the dependence of the MR of hybrid formats on layer thickness variation. Secondly we were interested in the influence of impurities on the MR.

The thicknesses of the layers appearing in some format are united in string form. Each string then corresponds to a unique system, and is referred to as a **configuration**. Consider for example the configuration: $\{\mathtt{a},\mathtt{b},\mathtt{c}\}$, meaning that the format consists of three layers (terminated by NM layers), with the layers having respective thicknesses $\mathtt{a}$,$\mathtt{b}$ and $\mathtt{c}$ in units of one atomic diameter. If some of the characters in the string are replaced by dots, *e.g.* $\{.,\mathtt{b},.\}$, this means that the thicknesses of the corresponding layers are varied simultaneously within a specified range. If the string features the subscript, $2\times$, as in $\{\mathtt{a},\mathtt{b},\mathtt{c}\}_{2\times}$ it means that the results of the configuration at hand also apply to its mirror image (the mirror image of $\{\mathtt{a},\mathtt{b},\mathtt{c}\}$ is $\{\mathtt{c},\mathtt{b},\mathtt{a}\}$). The thickness spectrum of

[1] For each member of the thickness spectrum: every barrier height produces an MR value, the average is taken over all such values.

some format is written also in string form. Consider the example $[a-b, c-d, e-f]$, meaning that the thickness of layer one varies from a to b, of layer two from c to d and of layer three from e to f.

The following estimations for the Fermi energies were used. In case we had Fe FM layers we set $E_F = 5.8\ eV$ (Fermi energy of Cr). In case of Co FM layers we set $E_F = 9.4\ eV$ (Fermi energy of Cu). Stearns [77] argued that inside Fe layers of tunneling junctions the effective mass of itinerant electrons equals the free electron mass: $m^* = m_e$. We will extend this assumption to Co FM layers and both types of NM layers. Inside barriers we will assume a lower mass, $m^* = 0.3\ m_e$. Together with the values of the Fermi energy we obtain from Eq. (3.31) the following length-scales (atomic diameter): $0.4\ \lambda_F$ inside Co and Cu layers; $0.3\ \lambda_F$ inside Fe and Cr layers; $0.2\ \lambda_F$ inside barriers.

8.3.1 1D Systems

The results on MR using the 1D static method of chapter 4 are presented in Figs.8.9-8.15. The values of the barrier potential $\mathcal{V}_{IS}$ were chosen to lie in an interval that covers all possible values extracted by inference from experiment. In FM=Fe systems we set the maximum barrier potential height at $1\ E_F$. In FM=Co systems we set the maximum barrier height $0.5\ E_F$.

The results on the MR as a function of the thickness of two of all FM layers are summarized in Figs.8.9-8.14. If in the figures, the configurations associated with some format are given exclusively in the top sub-figures (a and e) it means that the results in the sub-figures below them we obtained with the same configurations.

On comparing the results with that of the simple FIF format (Fig.8.3), we notice at once the more complicated evolution of the MR with the thickness of the FM layers. Since the thickness of the FM layers in the FIF were effectively infinite, this discrepancy has to be owed to the finiteness of the thicknesses of the FM layers in the hybrid formats. Another striking difference with the FIF format is that hybrid formats do not seem to show an unconditional increase in MR with the height of the barrier. Instead, hybrid formats seem to feature a contrast increasing property between the graphs of several configurations. Increasing the barrier height seems to either pull the graphs apart or make the peaks more pronounced. In general though, increasing the barrier height seems to have a positive effect of the MR. The oscillatory behavior in MR as a function of the thickness of the FM layers calculated by other authors [97] on the NFIFN format, is also found through our calculations, as Fig.8.9 shows.

The oscillatory behavior in MR with the thicknesses of its layer components however is not restricted to the NFIFN format but is observed in all formats. The cause of this very general feature is a very fundamental quantum mechanical one. Consider the format NFN, an FM layer of thickness a enclosed by two NM terminals. The 1D SE is solved by the standard procedure (see chapter 4). The situations with all the usual definition is depicted in Fig.8.7a. At the RHS the wave is transmitted into positive infinity. The coefficient of transmission $|t|^2$ is dependent on the position of the FN interface due to the matching requirement of the wave, as Fig.8.7b illustrates. It is precisely due to the oscillatory behavior of the wave inside the FM layer and the matching of the wave that the transmission amplitude t oscillates too. This is the essence of

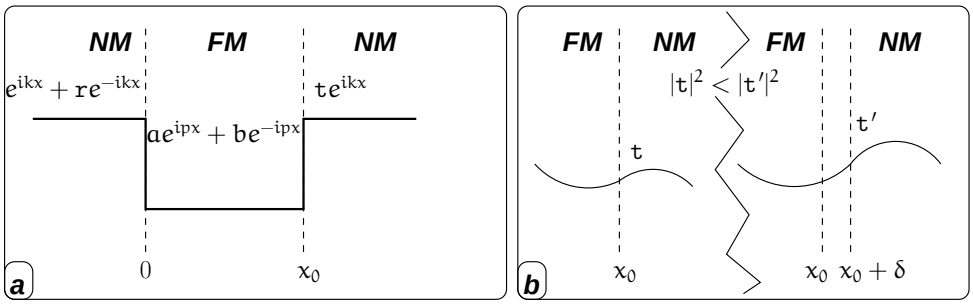

Figure 8.7: Illustration of the quantum mechanism ultimately responsible for the inherent oscillatory behavior of the MR in the thicknesses of its (non-insulating) layers. a. The SE-type of set-up of a NFN format, the amplitudes are fixed by the usual matching of function and derivative. b. A close-up at the FM-NM interface with coordinate x_0: the transmission amplitude t follows the oscillating wave within the FM layer. After increasing the size of the FM layer, by an amount δ_0, the transmission amplitude changes also.

the mechanism which ultimately is responsible for the observed oscillations in MR (the collective transmission gives conductance and conductance gives MR). The complexity of the nature of the oscillation in MR increases with the complexity of the configuration of the format. Note also that the layers defined in the format (only the FM-layer in this case) must account for at least one k−channel which does not have an imaginary wave-number (attenuation constant). If the layer becomes insulating the wave-numbers become attenuation constants and the transmission-coefficient loses its oscillatory quality. Thence from the above argument we might infer that the MR is oscillatory in the thicknesses of all conductive layers.

Let us have a closer look at Fig.8.9. First of all, regarding the LHS figures (FM=Co), the MR of the configurations $\{., 3, .\}$ remains more or less immune to barrier height increment. Secondly, the configurations with larger barrier widths respond with a decrease in MR on increasing the $\mathcal{V}_{\mathrm{IS}}$. From an application point of view, the plots given in e-h (FM=Fe) are perhaps more interesting. The configurations responsible for these figures allow for the formation of peaks in MR, which become ever more pronounced as the height of the barrier increases. A feature of both the Co and Fe systems is the phenomenon that the MR generally drops with increasing barrier width (see Fig.8.4). This feature is more clearly pronounced though for high barriers. In conclusion, in order to achieve maximal MR values one should stick to Fe layers, minimize the barrier width and maximize the barrier height (by finding suitable barrier-material, and by sharpening the interfaces). Then fine-tune the thickness of the FM layer to peak-value in MR. Since the first peak occurs for low FM thicknesses this suggests that the size of the systems may be held small.

Consider the format NFNFIFNFN, which might be conceived as the NFIFN format sandwiched by additional FM layers. We now simultaneously vary the thicknesses of either the outer FM layers or the inner FM layers. The results are given by Fig.8.10

(FM=Co) and Fig.8.11 (FM=Fe). The oscillating behavior of the MR is again well-represented for both the Fe and Co formats. First consider the variation of the thicknesses of the outer FM layers a-d of both figures. The figures suggest that the MR increases significantly on simultaneously increasing the width of the inner FM layers. This however is only apparent, we recall that the MR is oscillatory in the thicknesses of all conductive layers. Additional calculations, not presented here, indeed verify this behavior, by revealing a subsequent drop in MR on further increasing the widths of the inner FM layers. The variation of the thicknesses of the inner FM layers are given in e-h. Both FM=Fe as FM=Co formats show, aside from the oscillatory behavior, a pronounced peak development in MR. It is remarkable that the MR due to the FM=Co formats maintains a near-insensitive response to the increase in $\mathcal{V}_{\rm IS}$. In the FM=Fe formats on the other hand, we see ever more pronounced peaks emerging as $\mathcal{V}_{\rm IS}$ increases. Apart from the peak-behavior, both for FM=Fe and FM=Co systems there is no real noteworthy discrepancy between the evolutions of the MR from the several configurations ('spaghetti'). The results suggest that the MR drops with the barrier width. Through additional calculations, not presented here, it has been verified that indeed the MR increases as the width of the barrier decreases. In order to find the largest values of MR the directions given at the end of the discussion of the previous format also apply to this one.

The format NFNINFN can be thought to be constructed out of the NFIFN format by insertion of two NM layers adjacent to the IS barrier. The reason for doing so is explained in the text, see subsection 8.2.1 and Fig.8.2. The results on this format are given by Fig.8.12. The discrepancies between the FM=Co and FM=Fe formats are striking. First of all, while the Co formats show a typical single-peak[1] behavior the Fe formats maintain oscillatory behavior in MR. Also the MR again seems to be insensitive to increases in $\mathcal{V}_{\rm IS}$ for FM=Fe formats, while the MR in FM=Co formats increase strongly as a function of $\mathcal{V}_{\rm IS}$. Also the MR strongly increases with barrier width of FM=Co formats while slightly decreasing for the FM=Fe formats. Through additional calculations we have confirmed that this behavior perseveres for wider barriers and leads to spectacular gains in MR in FM=Co configurations. The MR in FM=Fe continues to decrease mildly as the barrier width increases. To achieve the highest MR values, one should choose FM=Co systems, make the barrier as wide as permitted (by the AF-coupling requirement) and fine tune the widths of the FM layer simultaneously until peak-value.

The large discrepancy between the MR values due to NFNIFN formats with either FM=Co or FM=Fe urges a closer analysis of the involved mechanisms. In subsection 8.2.1 we casually anticipated on the results to come by mentioning the so-called trapping effect. It was on the brink of completion of this thesis that we stumbled on a typical counter-intuitive manifestation of quantum mechanics. Consider Fig.8.2a. Intuitively we expect that the *total* transmission of the spin-up channel $\mathsf{T}_\uparrow$ exceeds that of the spin-down channel $\mathsf{T}_\downarrow$[2] since the potential barrier spin-up waves face is less than that of the spin-down waves. Secondly, we expect the polarization factor $\mathsf{T}_\uparrow/\mathsf{T}_\downarrow$ to be larger for the NFNINFN FM=Co format than the NFIFN FM=Co format to account for the

[1] The graphs have been cut-off at a thickness of 20 atomic diameters, extension to 30 add nothing new since the plots remain flat.

[2] The system is assumed to be in F-mode.

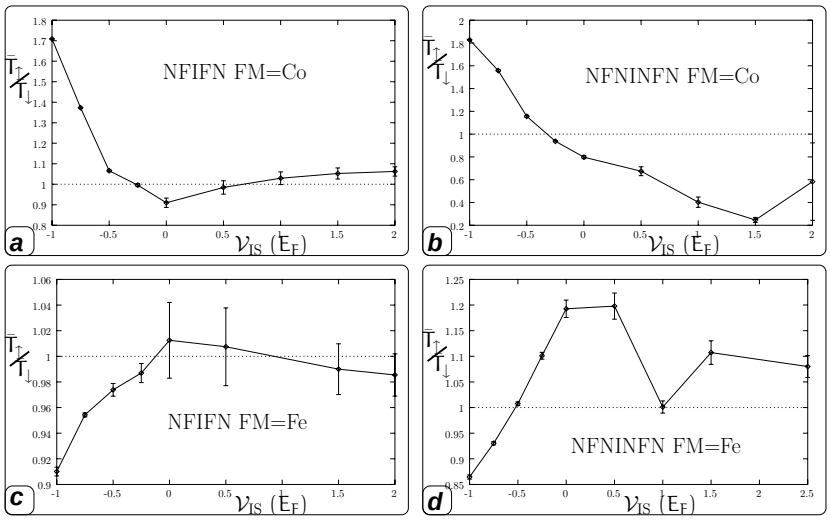

Figure 8.8: The average polarization factor $\bar{T}_\uparrow/\bar{T}_\downarrow$ as a function of the barrier height for the NFIFN formats at the LHS (a and c) and the NFNINFN formats (b and d). The thickness spectra averaged over are [5-15, 3-4, 5-15] and [5-15, 3, 3-4, 3, 5-15] for the NFIFN and NFNINFN formats, respectively.

tremendous elevations in MR for NFNINFN configurations as compared with the NFIFN. However, additional calculations reveal an equally unexpected and significant twist to this scenario. We have calculated the average of $T_\uparrow/T_\downarrow$ as a function of the barrier height for the NFIFN and NFNINFN formats, the results are given in Fig.8.8.

First we consider the FM=Co systems, Fig.8.8a and b. Intuitively, we expect the average of $T_\uparrow/T_\downarrow$ to be unconditionally greater than one. For low barrier heights this expectation is indeed verified, but on increasing $\mathcal{V}_{\rm IS}$ the polarization becomes significantly less than unity. That is, the polarization inverts. On comparing the sub-figures a and b, we notice that the inverting of polarization is more pronounced for the NFNINFN formats than the NFIFN formats. Though less severe, in Fig.8.8c and d a similar behavior is witnessed for the FM=Fe formats (with the role of spin-up and spin-dn interchanged). From this observation we infer that the NM layers surrounding the IS layer, has a decisive role in the inverting of the polarization. Regrettably, the reason for this remains obscure, and we do not hesitate to mention that further analysis on this peculiar quantum effect is needed to clarify its origin.[1]

The last format treated in this thesis arises when the previous format NFNINFN is sandwiched in between two FM layers (in turn attached to NM electrodes, of course). The results are presented in Fig.8.13 and Fig.8.14. We treat Fig.8.13 first. At the LHS of the figure, we notice, as $\mathcal{V}_{\rm IS}$ increases, the gradual appearing of a peak-like behavior

[1] We note that the inverting of the polarization factor is not an artifact due to our 1D implementation. Calculations on 2D systems reveal similar behavior.

in MR as a function of the thickness of the outer FM layers, yet preserving its oscillatory character (though of secondary role). This phenomenon is most pronounced with the $\{.,6,8,2,5,2,8,6,.\}$ configurations (pluses). This is an example of a format that shows an actual increase in MR with the barrier width. In general, the MR increases with the barrier height significantly and consistently. Notice however, that these gains in MR with the barrier height are not as spectacular as seen with the NFNINFN format. The addition of extra FM layers clearly reduced the spin-trapping mechanism to significant extent.

At the RHS of Fig.8.13 and Fig.8.14, where the thicknesses of the inner two FM layers are varied, we again notice the development of peaks as $\mathcal{V}_{\rm IS}$ increases. The configurations responsible for this behavior, once more, reveal a positive effect of increasing the barrier width. Apart from the peak-behavior, the evolutions of the MR again tend to spaghetti-like clustering. On regarding Fig.8.13, we at once notice the tendency of the MR evolutions to remain insensitive to an increasing $\mathcal{V}_{\rm IS}$.

In the last figure on 1D systems: Fig.8.15 we list the evolution of the MR with the height of the barrier $\mathcal{V}_{\rm IS}$. For each format, we give the seven configurations responsible for the highest average MR. For this purpose we have used the optimization algorithm of subsection 8.2.5. The general observation is that although often the MR is an increasing function of the barrier height, more than sometimes it is not. This is contrary to what one might expect based on the results for the FIF format (subsection 8.2.2) where the MR increases unconditionally with the barrier height. This seems to imply that in 'real' systems, *i.e.* systems that do not have infinitely wide layers, the behavior of the MR as a function of $\mathcal{V}_{\rm IS}$ is more complicated than simply non-decreasing.

We conclude the discussion on 1D systems by making some household remarks on the number of k_x-points needed to achieve proper convergence of the MR[1]. It turned out that tunneling systems require more points than GMR systems. In most formats a number of $\mathcal{O}(1000)$ sufficed for both Fe and Co FM layers. In the NFNINFN and NFNFNINFNFN formats with FM=Co, however, the number of required points is an increasing function of the barrier thickness and height. The number of required points ranged from $\mathcal{O}(10^4)$ to $\mathcal{O}(10^5)$.

8.3.2 2D Systems

The following symbols were used in the presentation of the results on 2D systems. The transverse dimension of the system L_y is given in units of the atomic diameter. The spreading in the impurity acceptance criterion σ as appearing in Eq. (6.22) basically determines the concentration of interface impurities. The smaller σ is chosen the more the impurities will be centered around interfaces.

The presence of impurities is quantified by using the concentration-concept similar to that used in the domain wall problem (chapter 5). The concentration or percentage is defined as the total area covered by impurities divided by the system size. In the results, the average values (ensemble size: 8 members, sub-ensemble size: 8-16 members) of the MR is given by small diamonds interconnected by solid lines (guides to the eye), the MR

[1]The longitudinal component of the momentum k_x ranges from zero to one (the Fermi momentum, see chapter 4).

due to individual ensemble members form the dotted lines (spaghetti) appearing at the background.

The results on 2D systems are condensed into Figs.8.16-8.19. We have performed the calculations for the two outer values of the allowed barrier-heights. In case the MR evolution behaves similar for both edge values, one might assume this also to be the case for intermediate values of $\mathcal{V}_{\mathrm{IS}}$. If there is a discrepancy, educated guesswork seems to be in place in the form of interpolation.

First consider Fig.8.16. At $\mathcal{V}_{\mathrm{IS}} = 0$ we clearly see an average negative consequence of increasing the impurity concentration. However, at $\mathcal{V}_{\mathrm{IS}} = 1.0\ \mathsf{E}_{\mathsf{F}}$ FM=Fe we notice a tendency of the MR to actually increase with the impurity density, although with large standard-deviations. The large standard-deviation in MR is due to the great fluctuations in conductance as a result to the great sensitivity of the conductance to the precise distribution of the impurities across the system.

Regarding Fig.8.17, we notice the following features. First, at $\mathcal{V}_{\mathrm{IS}} = 0.0\ \mathsf{E}_{\mathsf{F}}$ the average MR drops with the impurity concentration. At the higher barrier potential, we notice the formations of minima in the evolution of MR. This result is a consequence of the competition between the impurity MR-enhancing GMR mechanism (impurities in the FM-NM regions) and the usual TMR mechanism (impurities in the IS vicinity).

The general behavior displayed in Fig.8.18 is a uniform reduction in MR as a function of the impurity density. This response may be due to the spin-independent NM nature of the impurities within the barrier. It was stated in the text that the MR decreasing effect of NM impurities inside the insulating layer is stronger than that of FM impurities residing in the insulator.

The results given in Fig.8.19 are more promising. The addition of two FM layers to the sides of the NFNINFN format has a positive effect on the evolution of the MR (compare Fig.8.19 with Fig.8.18). In case of FM=Co at $\mathcal{V}_{\mathrm{IS}} = 0.5\ \mathsf{E}_{\mathsf{F}}$ we even observe the presence of a maximum, though with large standard deviations, at low impurity densities.

In the last part of the analysis of the 2D systems we have tried to find correlations between properties of the impurity distributions across the systems and the MR values. For example, one may hope to find a relation between high MR values and the preferred occurrence somewhere in the systems of one of the impurity species (FM, NM or IS). Besides the distribution of impurities the value of $\mathcal{V}_{\mathrm{IS}}$ proved to be rather influential in the evolution of MR with the impurity concentration. This is seen on noticing the discrepancies between sub-figures $\mathfrak{a}$ and $\mathfrak{b}$ for FM=Co and $\mathfrak{c}$ and $\mathfrak{d}$ for FM=Fe in Figs.8.16-8.19. The sensitive dependency of the MR on $\mathcal{V}_{\mathrm{IS}}$ makes it hard to find any correlations between favored impurity distributions and MR. Moreover, the lack of available data makes it even harder. It then comes as no surprise that we failed to reveal such correlations. Simply more data is needed.

8.3.3 1D vs. 2D

On comparing clean 1D systems with clean 2D systems, with identical configurations, we notice the occurrence of discrepancies in the values of MR. Table 8.1 shows a comparison of the MR values obtained with the static method (1D) with those obtained with the dynamic method (2D). The discrepancies are due to the differences in implementation

MR values (%), FM=Co						
Format, Config.	S1	D1	S1 / D1	S2	D2	S2 / D2
NFIFN						
$\{3,5,3\}$	8.3	5.7	1.5	4.6	6.1	0.75
NFNFIFNFN						
$\{6,5,3,5,3,5,6\}$	47	8.6	5.5	51	7.2	7.1
NFNINFN						
$\{5,3,4,3,5\}$	13	3.1	4.2	74	4.9	15.1
NFNFNINFNFN						
$\{3,6,4,2,5,2,4,6,3\}$	30	4.9	6.1	34	11	3.1
FM=Fe						
NFIFN						
$\{5,5,5\}$	7.5	4.9	1.5	4.8	2.0	2.4
NFNFIFNFN						
$\{6,5,3,5,3,5,6\}$	24	11	2.2	160	11	14.5
NFNINFN						
$\{5,3,3,3,5\}$	5.6	5.5	1.0	8.1	6.4	1.3
NFNFNINFNFN						
$\{4,6,4,2,3,2,4,6,4\}$	17	11	1.5	25	16	1.6

Table 8.1: The MR values of the 1D static ('S') method compared with the 2D dynamic ('D') method. The addition of '1' and '2' to 'S' and 'D' in the heading means that the potential is $\mathcal{V}_{\text{IS}} = 0$ in the former and either $\mathcal{V}_{\text{IS}} = 0.5\ \mathsf{E}_{\text{F}}$ (FM=Co) or $\mathcal{V}_{\text{IS}} = 1.0\ \mathsf{E}_{\text{F}}$ (FM=Fe) in the latter case.

of the static method and the dynamic method. In general, the discrepancy in FM=Co systems is more pronounced than the FM=Fe systems.

The first source of discrepancy is interference, or better, lack of interference due to the way the static method is implemented. In this method the solutions are calculated separately, solutions arising due to superposing a multiple of these separate solutions is ignored. Hence, the particular interference caused by all of the solutions treated as a whole is absent. This multiple wave-solution interference is however included in the dynamic method in a natural way.

The second source of discrepancy lies in the way the dynamic method differs in set-up from the static method. In the dynamic method, a wave-packet is set up at the LHS of the system and given momentum to propagate to the RHS. Due to this asymmetry the wave-packet is mostly reflected back and only a small (tunneling) fraction reaches the region beyond the barrier. Consider the NFNINFN FM=Co format showing the largest discrepancy between 1D and 2D results. The NM layers encompassing the IS layer, serving as spin-dependent wave traps, are held responsible for the great MR values seen in 1D systems. The reason that large MR values show up in 1D systems is that now both traps have a more symmetric effect. This lack of symmetry in 2D systems we hold responsible for the large calculated discrepancy.

To increase the trapping mechanism to full potential, with the dynamic method, would possibly be to maintain a continuous flow of incoming wave-function flux of which the transmitted and reflected fractions are continued to be absorbed at the terminals of

the system. In this way the traps will be able to, metaphorically speaking, fill themselves up with probability-intensity. Then the waves within the trap will ricochet back and forth at the exteriors of the trap. The mentioned modification in the dynamic method is, in fact, a step closer to the actual situation. In reality, electrons are continuously injected from external electrodes into the system and after a brief stay in the conductor they are either transmitted or reflected into the same electrodes.

To determine the relative contribution of both sources to the observed discrepancy would require to, ideally, ceiling off one source while opening the remaining source completely. The format which lends itself to that purpose is the NFIFN format, and to lesser extent the NFNFIFNFN format, where the trapping source is absent in the former case and hardly present in the latter. Unfortunately, a lack of available data prevents us from making substantial estimations. From the limited data, the least we can state is that interference seems to have a decreasing impact on the MR. Needless to say though, simply more data on more formats is needed.

8.3.4 Conclusions and Open Issues

The results seem to imply the following conclusions.

Concerning 1D systems:

1. For three out of four formats, we have verified the oscillatory behavior in the evolution of the MR with its layer widths, provided the layers have a non-insulating character. The one format which does not develop oscillatory behavior within the considered FM thickness range is the NFNINFN FM=Co format[1]. This format is responsible for the formation of well pronounced high-valued maxima in MR, this makes the format very eligible for application ends.

2. The effect of increasing the barrier width has a generally reducing effect on the MR, though it is less clear-cut than naively expected from the elementary FIF format. The exception again is provided by the NFNINFN, FM=Co format where the systems react with a strong increase in MR on increasing the width of the IS layer.

3. Increasing the barrier potential $\mathcal{V}_{\mathrm{IS}}$ turns out to have a strong format dependent and FM-type dependent effect on the MR. The response of the MR on increasing $\mathcal{V}_{\mathrm{IS}}$ is not at all unconditionally non-decreasing as the results on the FIF format suggest.

Concerning 2D systems:

1. The general tendency of hybrid formats, in agreement with expectations based on the FIF format, is to show a decay of MR with the impurity density. A possible exception to this general tendency is perhaps best given by the NFNFNINFNFN FM=Co format, where, for the given configuration, the average MR even develops a maximum as a function of impurity concentration. From the point of view

[1] It is, of course, possible that the periods of oscillation fall well out of the considered range.

of technological applications, where the MR levels need to be conserved, this format might be the best candidate. We stress, however, that these are preliminary findings, simply more data is needed before drawing any general conclusions.

2. The erratic character of the evolution of the MR seen in individual systems and its strong dependence on $\mathcal{V}_{\mathrm{IS}}$ makes it hard, to say the least, to find correlations between certain properties of impurity distributions and the value of MR.

3. The differences in the calculated MR values obtained with the 1D static method and the 2D dynamic method suggest two sources of discrepancy. The dynamic method includes multi-wave interference-effects but does not properly reflect the mentioned spin trapping effect (see subsection 8.2.1 and the discussion in subsection 8.3.3). On this matter, the static method is precisely its antagonist.

We end this chapter, and hence this thesis, by giving a list of issues which have not been addressed yet.

1. Due to the diversity of the concept of hybrid formats many formats, such as double (triple etc.) barrier systems, and their properties remain unexplored.

2. The results obtained on impure 2D systems is insufficient to expose any general behavior, except in a confirming way. The general behavior may be extracted only after many equivalent systems have been analyzed.

3. The angular behavior of the MR was not treated here. This, however, can be done without further modification of the model in a way similar to the angular behavior of GMR systems.

4. A feature not included in the model is the provision of the FM impurities with a paramagnetic flavor. As was shown in chapter 6 this has a destructive effect on the MR. Applied to the hybrid formats, the GMR effect on the MR will shift from constructive to destructive and hence the MR will drop even faster with the impurity concentration.

5. We are aware of the necessity to have an anti-ferromagnetic coupling between the FM electrodes in the here assumed multi-layer type of TMR, but was disregarded nonetheless. Respecting this condition will put severe restrictions on the allowed distances between the FM layers, and hence possible configurations. A way out to this problem is provided by the alternative of spin-valve type of MR (see chapter 7) where the FM coupling is less important and can even be irrelevant. A technical prerequisite (which might be difficult?) then is to properly parameterize the band parameters of the different FM layers.

6. In order to give a better representation of the spin-trapping effect we should modify the dynamic model. To acknowledge the continuous flow of emitted current into the system we might continuously initialize new waves at the emitting side of the system throughout the simulation time. This modified model might also successfully be applied to CIP-GMR systems (chapter 6).

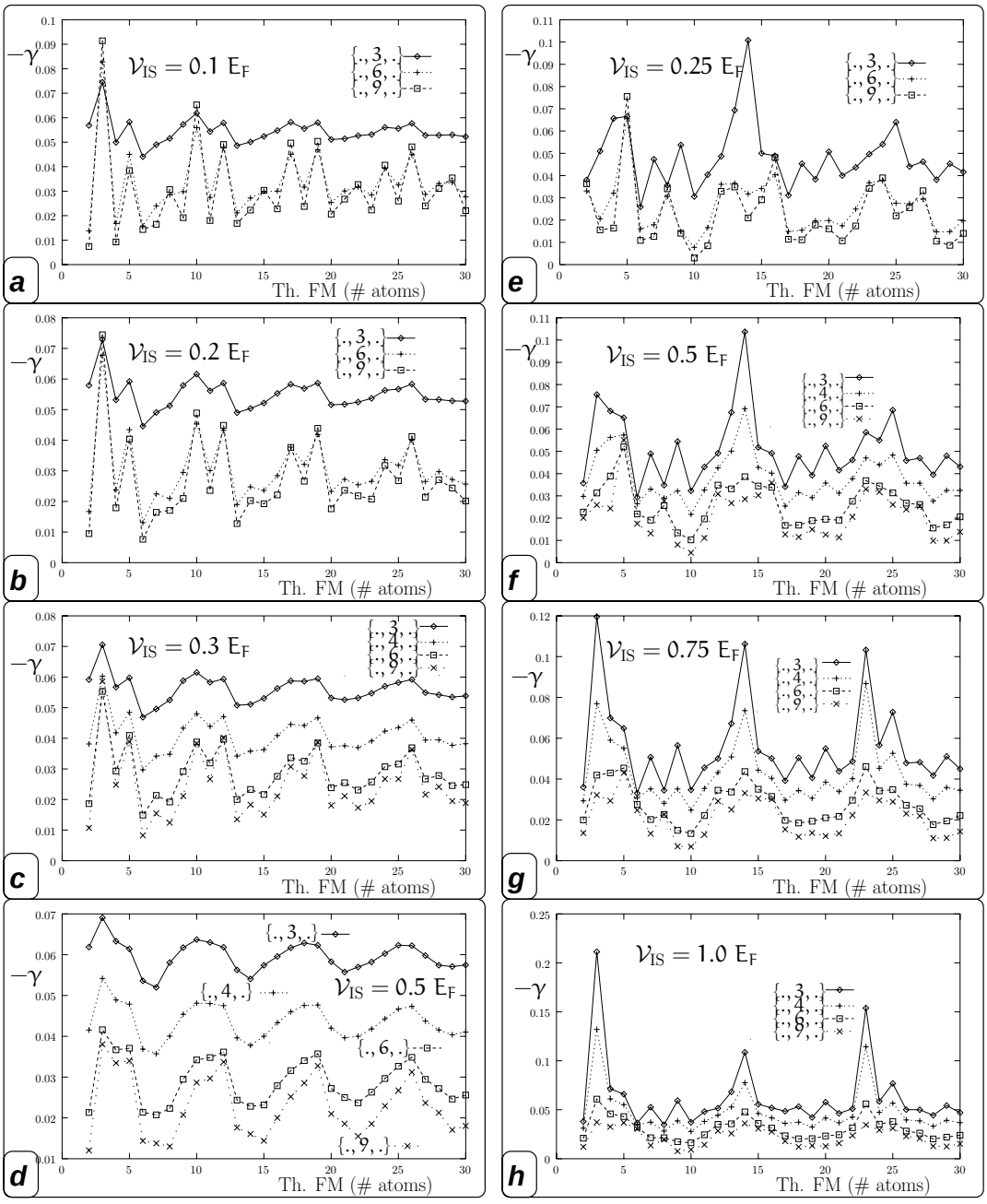

Figure 8.9: The MR, of the format NFIFN, as a function of thicknesses of the outer FM layers (Th. FM) for several barrier-potentials (the thicknesses are varied simultaneously). In a-d the FM layers are Co-like, in e-h Fe-like.

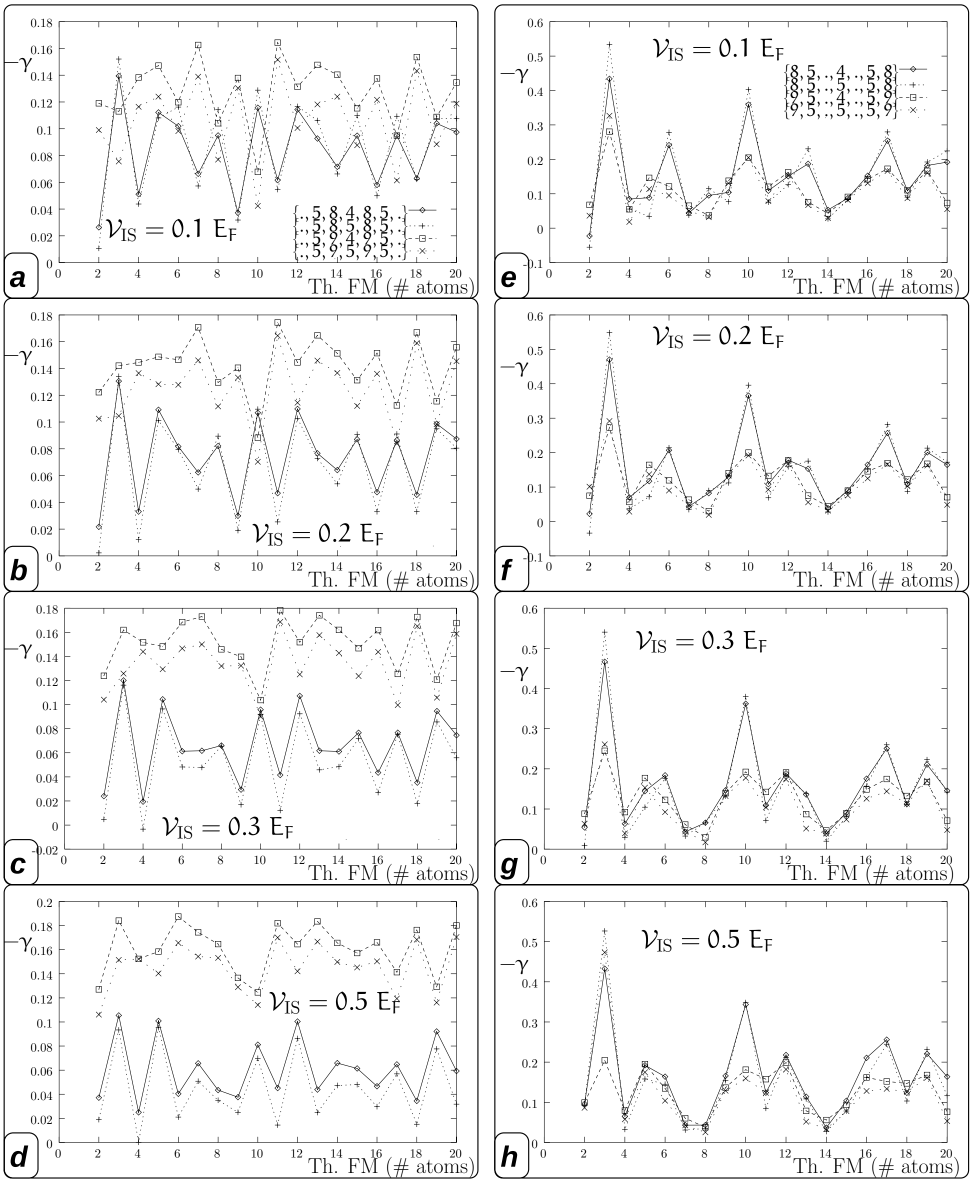

Figure 8.10: The MR, of the format NFNFIFNFN, as a function of thicknesses of two of the four FM layers for several barrier-potentials. The FM layers are all Co-like.

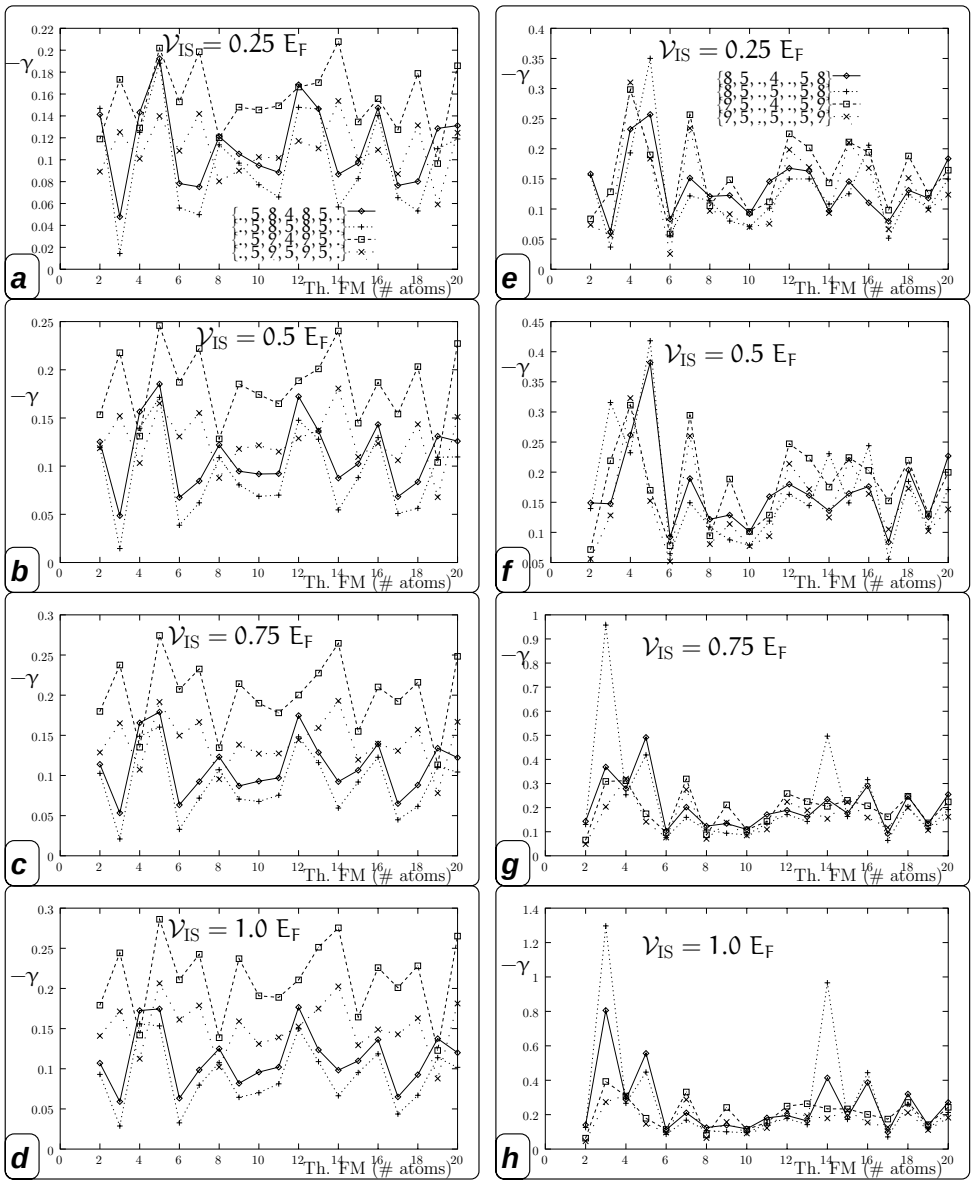

Figure 8.11: The MR, of the format NFNFIFNFN, as a function of thicknesses of two of the four FM layers for several barrier-potentials. The FM layers are all Fe-like.

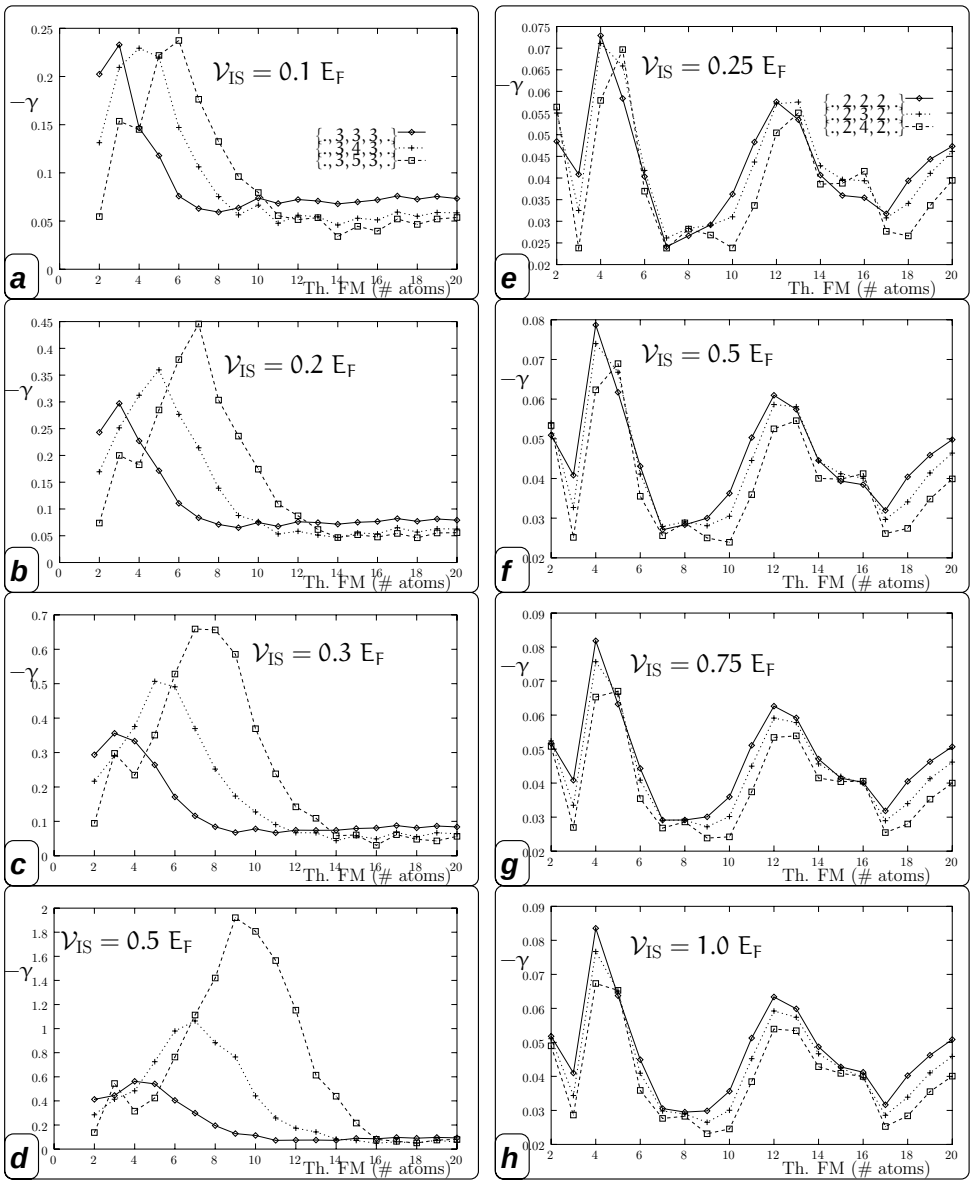

Figure 8.12: The MR, of the format NFNINFN, as a function of thicknesses of the outer FM layers for several barrier-potentials. In a-d the FM layers are Co-like, in e-h Fe-like.

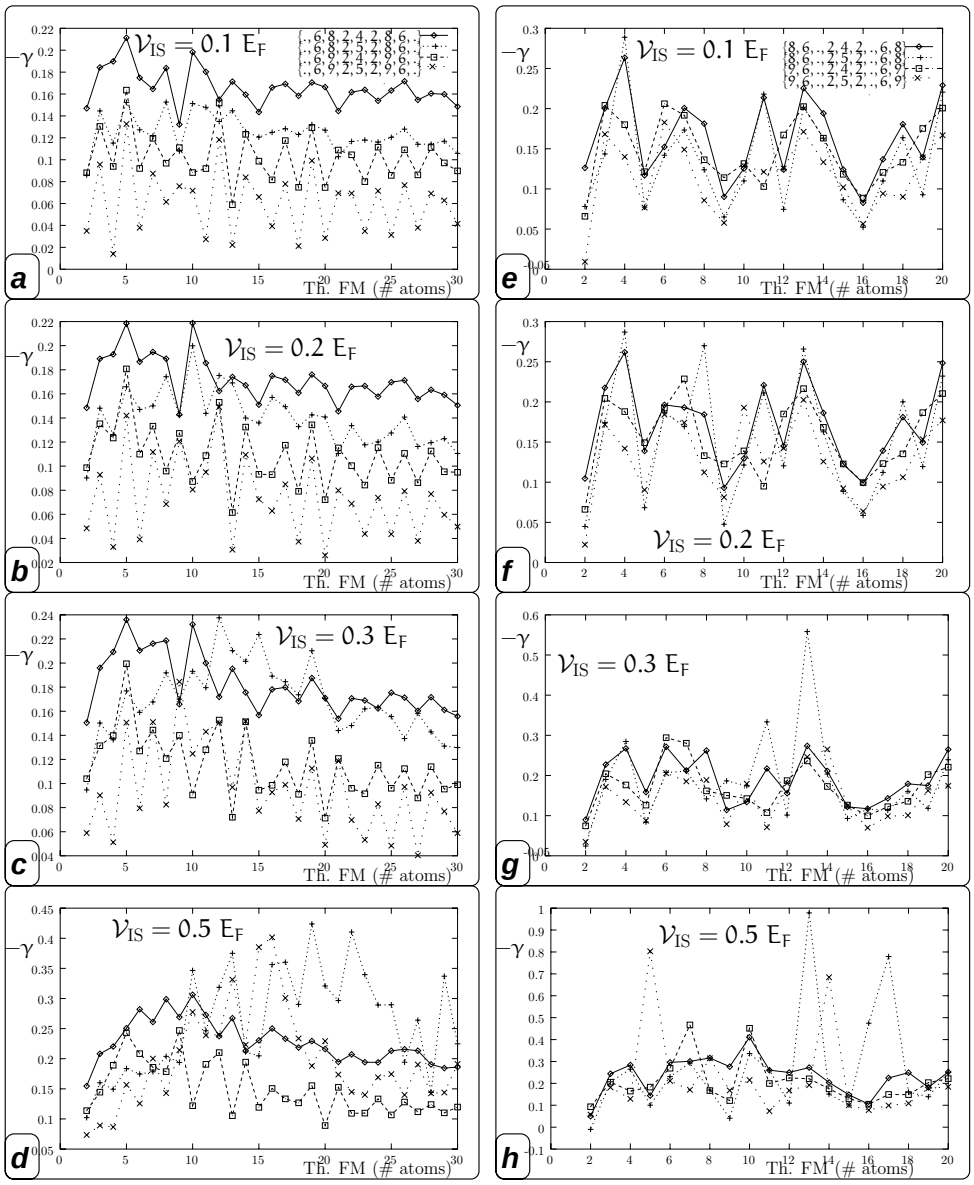

Figure 8.13: The MR, of the format NFNFNINFNFN, as a function of thicknesses of two of the four FM layers for several barrier-potentials. The FM layers are all Co-like.

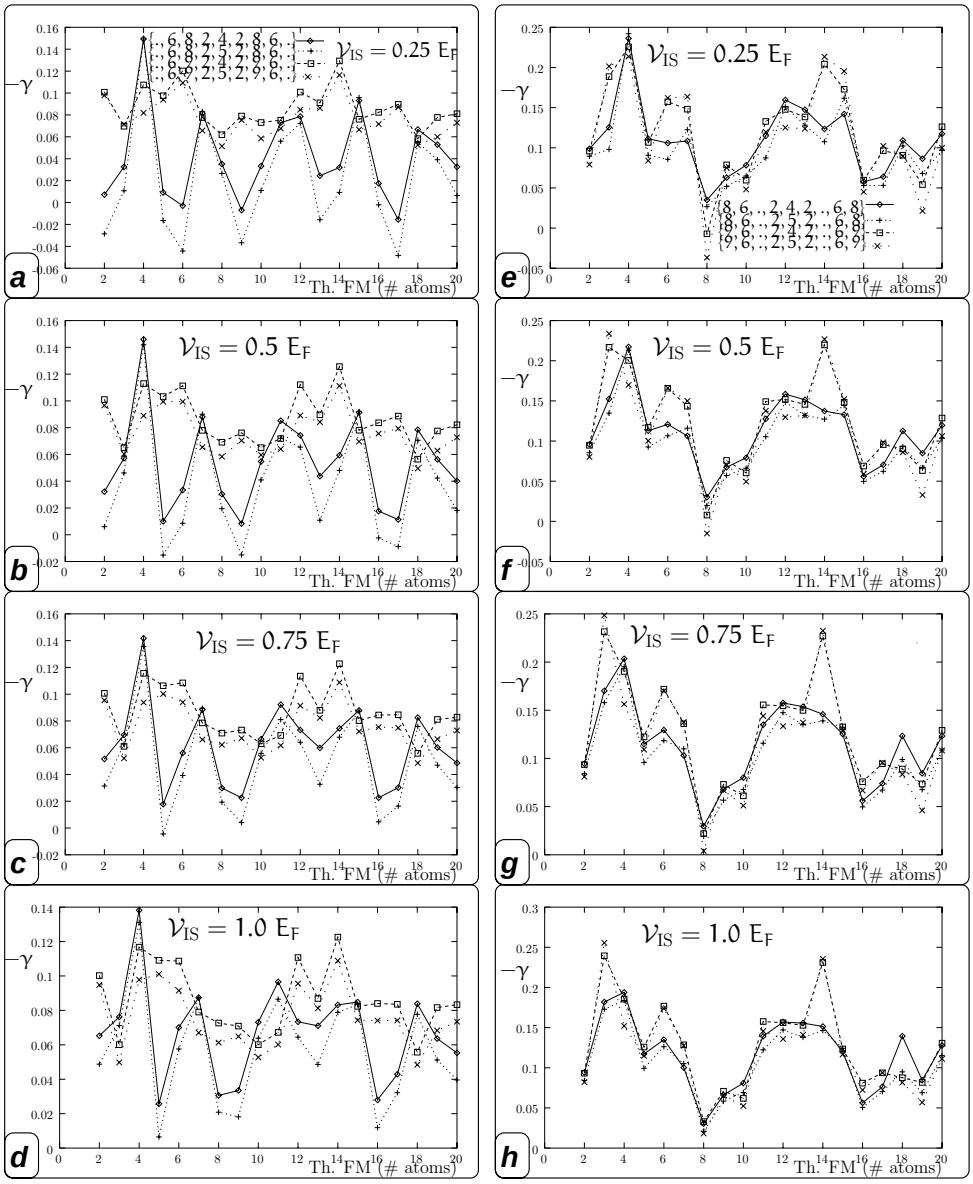

Figure 8.14: The MR, of the format NFNFNINFNFN, as a function of thicknesses of two of the four FM layers for several barrier-potentials. The FM layers are all Fe-like.

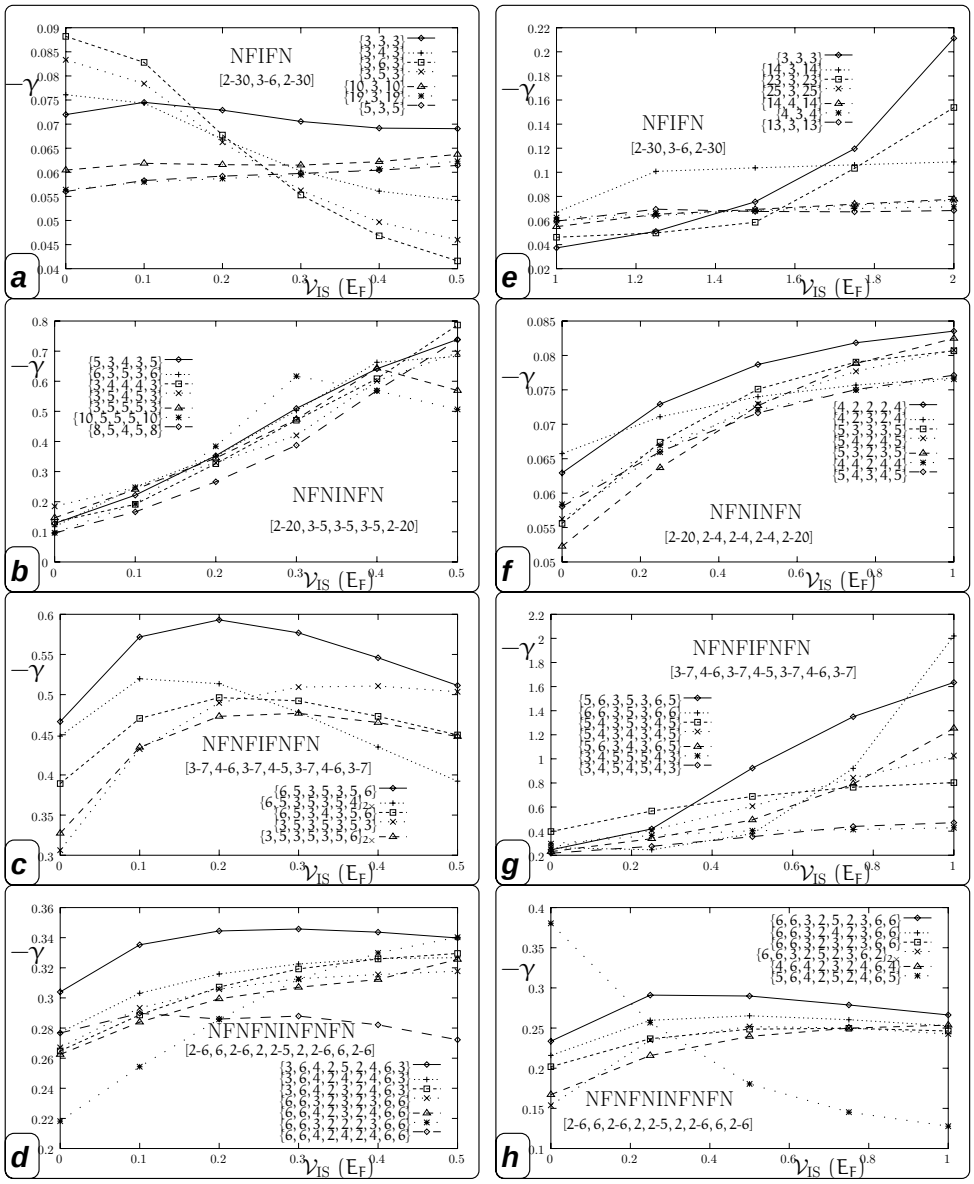

Figure 8.15: The MR as a function of the barrier height $\mathcal{V}_{\rm IS}$. Shown here are the top-7 (highest average MR) members from each given thickness spectrum of the corresponding format. In a-d we have FM=Co, in e-h FM=Fe.

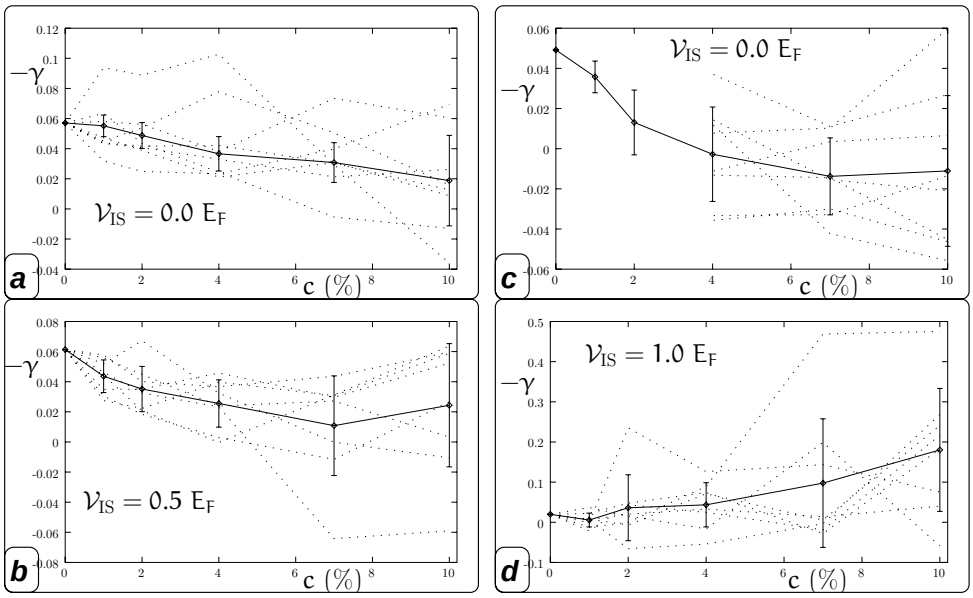

Figure 8.16: The calculated annealing MR behavior for 2D systems of the format NFIFN. In a&b the FM layers are Co-like, configuration: $\{3, 5, 3\}$. In c&d the FM layers are Fe-like, configuration:$\{5, 5, 5\}$. Transverse dimension: $L_y = 40$ atoms, spreading: $\sigma = 3$ atoms.

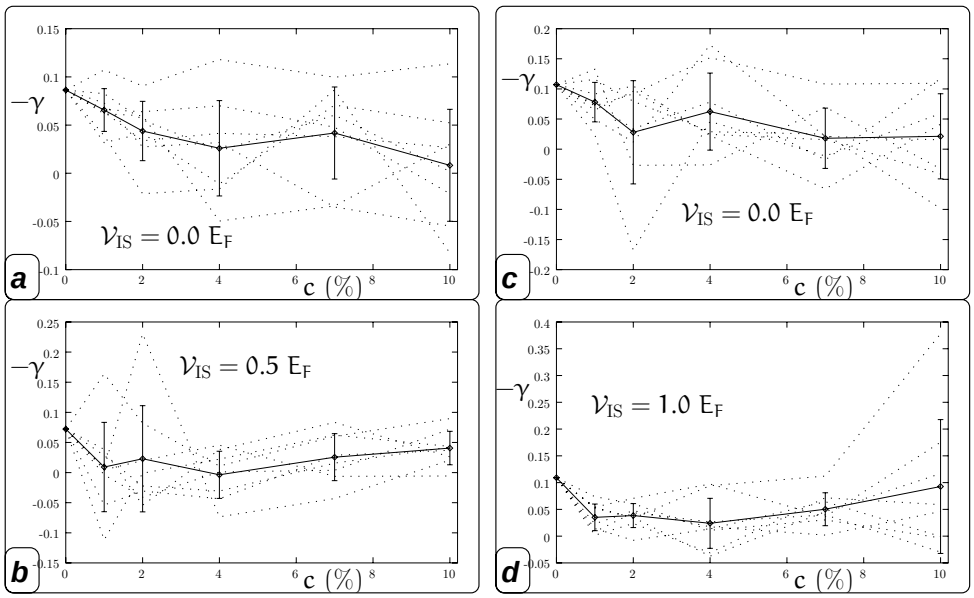

Figure 8.17: The calculated annealing MR behavior for 2D systems of the format NFNFIFNFN. In a&b the FM layers are Co-like, configuration: $\{5, 6, 3, 5, 3, 6, 5\}$. In c&d the FM layers are Fe-like, configuration:$\{5, 6, 3, 5, 3, 6, 5\}$. Transverse dimension: $L_y = 20$ atoms, spreading: $\sigma = 3$ atoms.

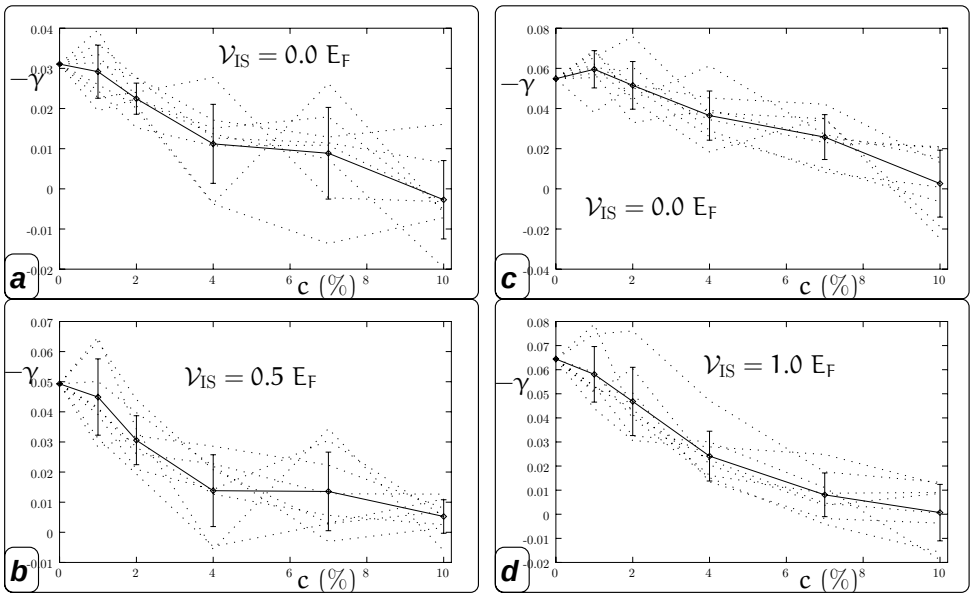

Figure 8.18: The calculated annealing MR behavior for 2D systems of the format NFNINFN. In a&b the FM layers are Co-like, configuration: $\{5, 3, 4, 3, 5\}$. In c&d the FM layers are Fe-like, configuration:$\{5, 3, 3, 3, 5\}$. Transverse dimension: $L_y = 20$ atoms, spreading: $\sigma = 1$ atoms.

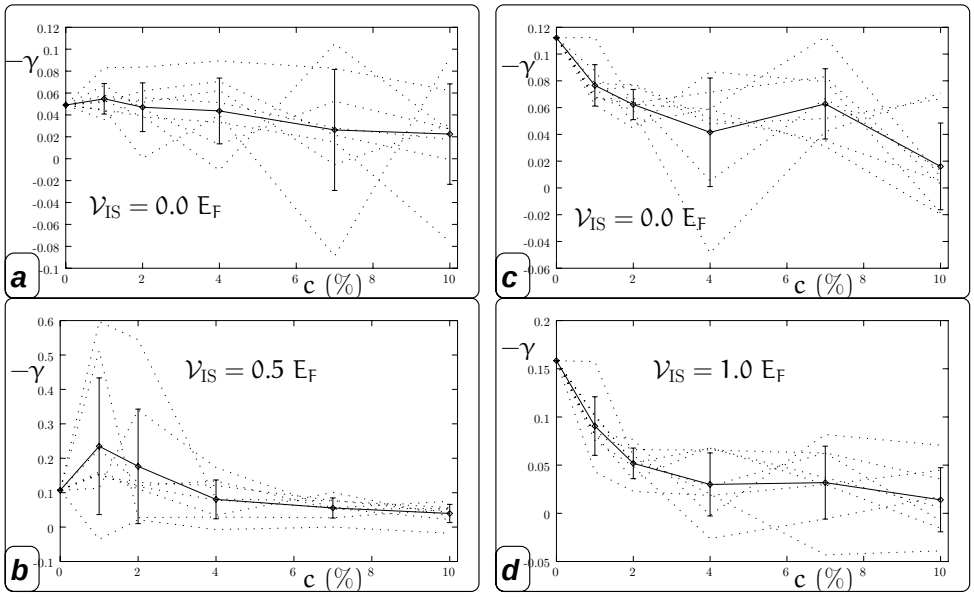

Figure 8.19: The calculated annealing MR behavior for 2D systems of the format NFNFN-INFNFN. In a&b the FM layers are Co-like, configuration: $\{3, 6, 4, 2, 5, 2, 4, 6, 3\}$. In c&d the FM layers are Fe-like, configuration:$\{4, 6, 4, 2, 3, 2, 4, 6, 4\}$. Transverse dimension: $L_y = 20$ atoms, spreading: $\sigma = 1$ atoms.